Mikhail Krakhalev, Vitaly Sutormin, Oxana Prishchepa,
Anna Gardymova, Alexander Shabanov, Wei Lee, Victor Zyryanov

7 Liquid crystals doped with ionic surfactants for electrically induced anchoring transitions

Abstract: Two conceptually different approaches can be used to operate liquid crystal (LC) materials. One approach is based on numerous variants of the Frederiks effect, which enables the LC reorientation caused by external stimuli without a change of boundary conditions. All modern optoelectronic LC devices function on the basis of this effect. The other exploits the anchoring transitions through the modification of the surface anchoring strength with a change in the tilt and (or) azimuthal anchoring angle(s) under the external influence (temperature, irradiation, electric field, and so on). This chapter provides an overview of a novel method to control LC materials by electrically induced anchoring transitions. The key element entailed in our method is an ionic surfactant dissolved in LC. The surfactant is adsorbed partially on the LC cell substrate, thus specifying certain boundary conditions. Its concentration at the interface varied under the action of DC electric field resulting in the modification of the surface anchoring. Following this, changing boundary conditions makes the whole bulk of LC reoriented into a different state. The modification of boundary conditions can be realized in both the normal and inverse modes, depending on the content of the ionic surfactant in LC. This ionic-surfactant operation (ISO) method is applicable to both polymer-dispersed LC (PDLC) films and nematic and cholesteric LC layers. Dynamical parameters of the electro-optical response of various LC structures are considered. Response times of the ISO optical cells of twisted -nematic layers are decreased to tens or hundreds of milliseconds at some volts of applied electric voltage. The implementation of the ISO method into operating PDLC devices allows observations of the novel bistability effects in cholesteric droplets. The most impressive feature of the ISO method is the possibility to reorient LC with dielectric anisotropy $\Delta\varepsilon$ of any sign and value, including $\Delta\varepsilon = 0$.

Acknowledgments: Wei Lee acknowledges the financial support from the Ministry of Science and Technology, Taiwan, through grant nos. NSC 98-2923-M-033-001-MY3, NSC 103-2923-M-009-003-MY3, and MOST 106-2923-M-009-002-MY3, which has enabled his intent and decade-long collaboration with the Russian team led by Victor Ya. Zyryanov.

https://doi.org/10.1515/9783110584370-007

7.1 Introduction

Impetuous development of nanotechnologies renders the study of surface phenomena increasingly topical. The effects occurring at the interface between two media, of which one is liquid crystal (LC), are quite specific (Barbero and Evangelista, 2006; Blinov et al., 1987). The most spectacular feature is that the comparatively weak surface anchoring forces not only can orient the near-surface LC molecules but also can affect the director configuration in a region offset by a few tens of microns from the interface. This property is basic to the functioning of all modern electro-optical LC devices because it allows the desired orientational structure to be organized in an LC layer through the formation of appropriate boundary conditions. An external electric field reorients LC in its bulk but does not markedly change the interface structure. This transformation is typical for the numerous variants of the classical Frederiks effect (Blinov, 1983; Freedericksz and Zolina, 1933). After switching off the field, the forces of surface interaction restore the initial director configuration in the bulk of LC.

A conceptually new approach was developed on the basis of the so-called local Frederiks transitions (Blinov et al., 1987; Dubois-Violette and De Gennes, 1975) or anchoring transitions consisting in the transformations of the director orientation in the bulk as a result of a change in the balance of the orienting actions of the different surface forces. A typical example is the reorientation of a nematic layer screened from a crystal substrate by a thin amorphous film (Blinov et al., 1984; Ryschenkow and Kleman, 1976). The orienting actions of the film and substrate must be different, for example, planar and homeotropic. The variation in the film temperature (Ryschenkow and Kleman, 1976) or the film thickness (Blinov et al., 1984) changes the balance of the orienting forces and, thus, initiates the reorientation of LC layer. In practice, the methods of modifying boundary conditions by an electric field are most essential. For this purpose, for example, the substrates coated with a ferroelectric LC polymer were used by Komitov et al. (2005). After a change in the polarity of the applied voltage, the azimuthal director reorientation in the LC polymer induces the respective orientational transformation in the bulk of the nematic LC (NLC) bordering such a substrate.

There is another opportunity to realize the electrically controlled anchoring transition based on the ionic-surfactant method. In 1972, Proust and his colleagues observed an interesting phenomenon when the concentration of adsorbed cationic surfactant cetyltrimethylammonium bromide (CTAB) influences dramatically the LC surface anchoring (Proust and Ter Minassian Saraga, 1972). They showed that at low content of the surfactant at interface, a planar (tangential) anchoring is formed (Figure 7.1). At high content of CTAB admixture, the surface anchoring becomes homeotropic (perpendicular). This result underlay the technique offered by Petrov and Durand (1994) to implement an electrically controlled change of boundary conditions in the planar nematic layer with an ionic surfactant preliminarily deposited on

substrates of the LC cell. However, an anchoring transition was not realized in the pure form because electrohydrodynamic instability was the dominant effect.

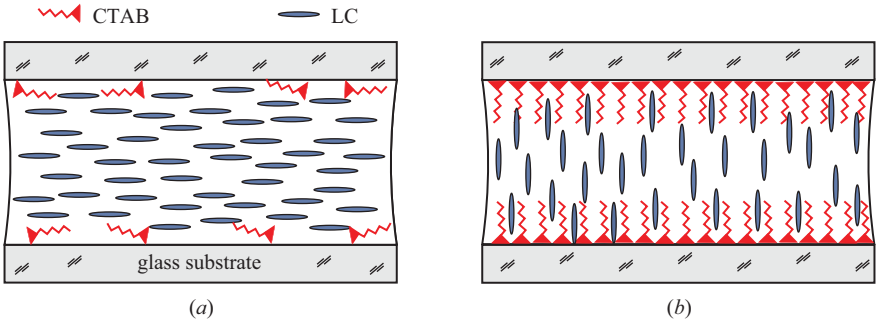

Figure 7.1: A planar anchoring of LCs is formed at low content of CTAB molecules at interface (a). An increase in CTAB concentration leads to the formation of a homeotropic surface anchoring (b).

In our experiments, the ability of CTAB to dissolve slightly in LC and dissociate into ions was used. A method of controlling the LC structure which is based on the modification of surface anchoring by electric-field-driven ionic surfactant was implemented for the first time for nematic droplets (Zyryanov et al., 2007b). We believe that the development of this approach can lead to the creation of principally new LC materials capable of significantly expanding the functional possibilities of optoelectronic devices.

This chapter reviews the previous works of authors primarily done on the development of LC materials with electro-optical characteristics controlled using ionic-surfactant method.

7.2 Polymer-dispersed liquid crystal films controlled by ionic-surfactant method

7.2.1 Composition and sample preparation

We used the following material components for the preparation of polymer-dispersed LC (PDLC) films (Figure 7.2): well-known nematics 4-*n*-pentyl-4′-cyanobiphenyl (5CB) with dielectric anisotropy $\Delta\varepsilon = +13.3$ at 25 °C (Bradshaw et al., 1985) and 4-methoxybenzylidene-4′-*n*-butylaniline (MBBA) $\Delta\varepsilon = -0.54$ at 25 °C (Klingbiel et al., 1974), polymers polyvinyl butyral (PVB) and polyvinyl alcohol (PVA) specifying the tangential (planar) boundary conditions, glycerin as a plasticizer for PVA, cationic surfactant CTAB, and a chiral additive cholesteryl acetate (ChA) to prepare cholesteric LCs (ChLCs).

The samples of PDLC films based on PVB were prepared by the solvent-induced phase separation (SIPS) method (Crawford and Zumer, 1996; Zharkova and Sonin, 1994). A mixture of LC 5CB and polymer PVB taken in a weight ratio of 1:1 with the surfactant CTAB of varied concentration was dissolved in ethanol. The solution was poured on the substrates with indium–tin -oxide (ITO) electrodes and dried. After ethanol evaporation, the polymer film was formed with LC droplets dispersed in it. The film thickness and LC droplet's size were specified by the conditions of the SIPS process (the ratio of the material components and rate of evaporation).

The emulsification method was used to prepare the samples of PDLC films based on polymer PVA (Drzaic, 1995). At that, a nematic LC doped with the cationic surfactant CTAB was emulsified into an aqueous solution of the film-forming PVA polymer plasticized with glycerin. The ratio of used components varied according to each case under consideration.

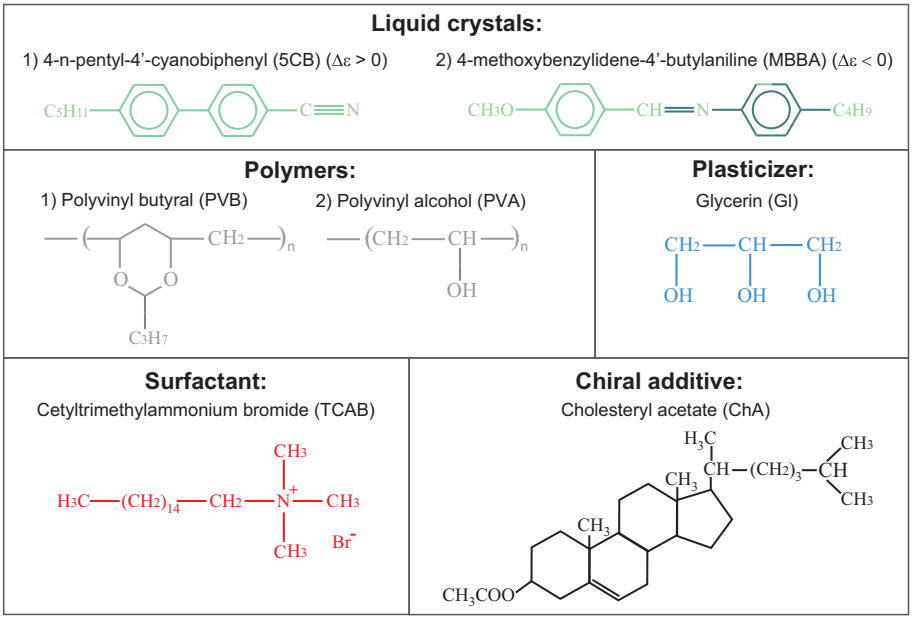

Figure 7.2: Material components to prepare liquid crystal/surfactant/polymer composite structures.

7.2.2 Normal mode of the electrically induced anchoring transition in nematic droplets

CTAB was used as an ion-forming surfactant providing normal (homeotropic) boundary conditions (Cognard, 1982; Proust and Ter Minassian Saraga, 1972) at a certain concentration. When dissolved in LC, this compound dissociates into a negatively

charged Br^- ion and a positive CTA^+ ion. The surface-active properties of CTAB are only due to the cations, which when adsorbed at the interface can form molecular layers in which the long alkyl chains $C_{16}H_{33}$ are aligned perpendicular to the surface.

To study the textural changes and orientational structures (director configurations) in nematic droplets, a PDLC cell with in-plane applied electric field was prepared (Figure 7.3). The gap between the electrode strips at the substrate was 100 μm. Experiments were performed with composite films that are uniaxially stretched. Monopolar rectangular electrical pulses of 1-s duration with an amplitude varying from 0 to 1,000 V were applied to the electrodes. The texture patterns of the LC droplets were observed using a polarizing optical microscope (POM) in the geometry of crossed polarizers and with the analyzer turned off.

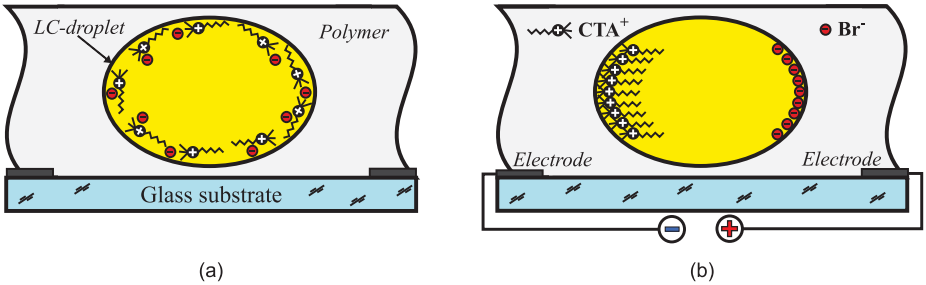

Figure 7.3: Scheme of PDLC cell with a CTAB dissolved in the nematic droplets. The content of CTA^+ ions adsorbed at the droplet surface is not enough to block the orienting forces of polymer walls and specify homeotropic anchoring; therefore, the tangential (planar) boundary conditions are realized in the initial state (a). When DC electric field is switched on, the CTA^+ ions are localized in the part of droplet near the cathode and modify an anchoring at the interface from tangential to homeotropic (b).

The droplets of 5CB nematic dispersed into a pure PVB matrix with the tangential anchoring are characterized by a bipolar director configuration (Prishchepa et al., 2005). The texture patterns of the nematic droplet and the corresponding director configurations typical for the studied composite film are demonstrated in Figure 7.4. One can see that the orientational structure of the droplets is bipolar with two surface point defects – boojums – in initial state (Figure 7.4(a)), evidencing the tangential anchoring for the chosen concentration of the CTAB surfactant.

In the geometry of crossed polarizers (Figure 7.4(a), top row), two extinction bands originate from the defects located at the ends of the droplet's major axis and expand gradually shading the central part of the droplet. The bipolar director configuration in the central section of the nematic droplet is schematically shown by the dashed lines at the bottom row of Figure 7.4(a).

In the geometry with the turned-off analyzer (Figure 7.4(a), middle row), two boojum defects (Volovik and Lavrentovich, 1983) are seen as dark spots at the ends

of the major axis of a prolate droplet. This became possible because of the large gradient of the refractive index near the defects and, hence, intense local light scattering. For the same reason, the parts of the droplet boundary are also clearly seen, where the light polarization coincides with the local director orientation. The gradient of the extraordinary refractive index of nematic droplet, $n_{||}$, and the refractive index of polymer, n_p, $\Delta n = n_{||} - n_p$, is maximal at these points. The boundary sections with the orthogonal arrangement of the director and light polarization are defined less sharply because the gradient $\Delta n = n_{\perp} - n_p$ is minimal in this region, where $n_{\perp}$ is an ordinary refractive index of nematic droplet.

The droplet's pictures corresponding to the end of the pulse when the electric vector is directed rightward are shown in Figure 7.4(b). Analysis of the corresponding textures shows that the right boojum decomposes in this case, and the director lines are almost uniformly aligned with the applied field at right half of the droplet. At the left half, the texture is unchanged suggesting that the initial director configuration is retained. The orientational structure corresponding to the new state of the droplet is shown at the bottom row of Figure 7.4(b). Of the previously described structures, the field-free monopolar structure (Prishchepa et al., 2005) of the lecithin-doped nematic droplets is a closest analogue to this configuration. The reversal of the field direction (Figure 7.4(c)) induces symmetric changes in textures: the left defect decomposes, while the initial director distribution in the right half of the droplet is retained.

In this situation, the orienting action of the external field on the LC bulk is not crucial. The concentration of the ionic impurity in the samples was so high that the applied field was almost fully screened inside the droplet by the field of spatially separated ionic charges (Barannik et al., 2005).

The observed transformation of the orientational structure in the LC droplet can convincingly be explained by the ion rearrangement (Figure 7.3). Under the action of the external field, the surface-active cations are concentrated near the droplet boundary close to the cathode forming here the close-packed CTA^+ layers with alkyl chains aligned perpendicular to the interface (Figure 7.3(b)). In the LC droplets studied, the fraction of CTAB was ~0.5 wt% or ~2.6×10^{-12} g for a spherical droplet with a radius of 5 μm. Regarding the molecular weight $M_{CTAB} = 6.04 \times 10^{-22}$ g, such a droplet contains ~4.3×10^9 CTAB molecules. The projection of a homeotropically arranged CTA^+ cation onto the interface is about 0.15×10^{-18} m^2 for the straightened *trans*-conformation of the alkyl chain. With these parameters, four close-packed monolayers of the CTA^+ cations can form at the half of droplet surface close to the cathode. Clearly, the number of monolayers is maximal at the point closest to the cathode and it decreases gradually with distance from this point. For comparison, the critical number of polar monolayers of stearic acid (whose molecules are similar in size and shape to the CTA^+ ions) in 5CB LC is two, while the number of nonpolar bilayers is ten (Blinov et al., 1984). In our case, the cationic monolayers screen also the orienting action of the PVB matrix and change the surface anchoring from tangential to homeotropic.

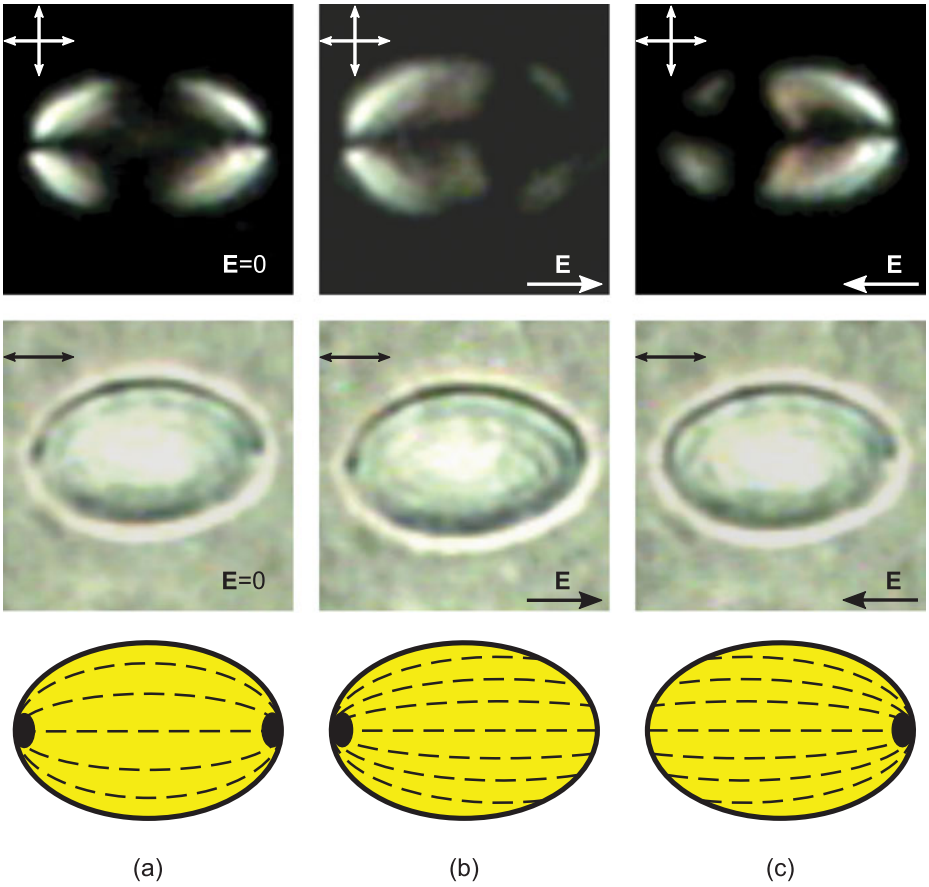

Figure 7.4: POM images of a nematic droplet between crossed polarizers (top row), with the turned-off analyzer (middle row), and the corresponding director configurations (bottom row). The electric field is switched off (a). The electric field $U = 280$ V is directed along the droplet's major axis to the right (b) and to the left (c). A gap between the electrodes is 100 μm, and a size of droplet's major axis is 13 μm. The polarizer orientations here and in the following figures are shown by the duplex arrows.

The modification occurs locally at the boundary area closest to the negative electrode. At a distance from it, the concentration of the cationic surfactant decreases and the anchoring angle θ (between the LC director and the normal to the surface) can change gradually from 0 (in the point of the destroyed defect) to 90° at the boundary area adjacent to the minor axis of the ellipsoidal droplet. After the field reversal, the CTA^+ ions transfer to the left half of the droplet and form there homeotropic anchoring. After a cation departure, the tangential boundary conditions and the surface boojum are restored at the right half of the droplet. As shown, the local increase in concentration of the Br^- anions does not cause the surface anchoring transition.

The orientational structure transformations occurring in LC droplet under electric field applied perpendicular or nearly perpendicular to the bipolar axis (Figure 7.5) are explained in a similar manner. In this case, the curved monopolar structure is formed (Figure 7.5(b) and (c)). One of the boojums is retained in the right half of the droplet in Figure 7.5(b) and in the left half in Figure 7.5(c). The other boojum decomposes, and the director lines deflect either upward (Figure 7.5(b)) or downward (Figure 7.5(c)) and crop out at the surface area saturated with the cations, where the boundary conditions become homeotropic and nearly homeotropic. At the opposite side of the droplet, where the Br anions are localized, the tangential anchoring is retained, as in the case shown in Figure 7.4(b) and (c).

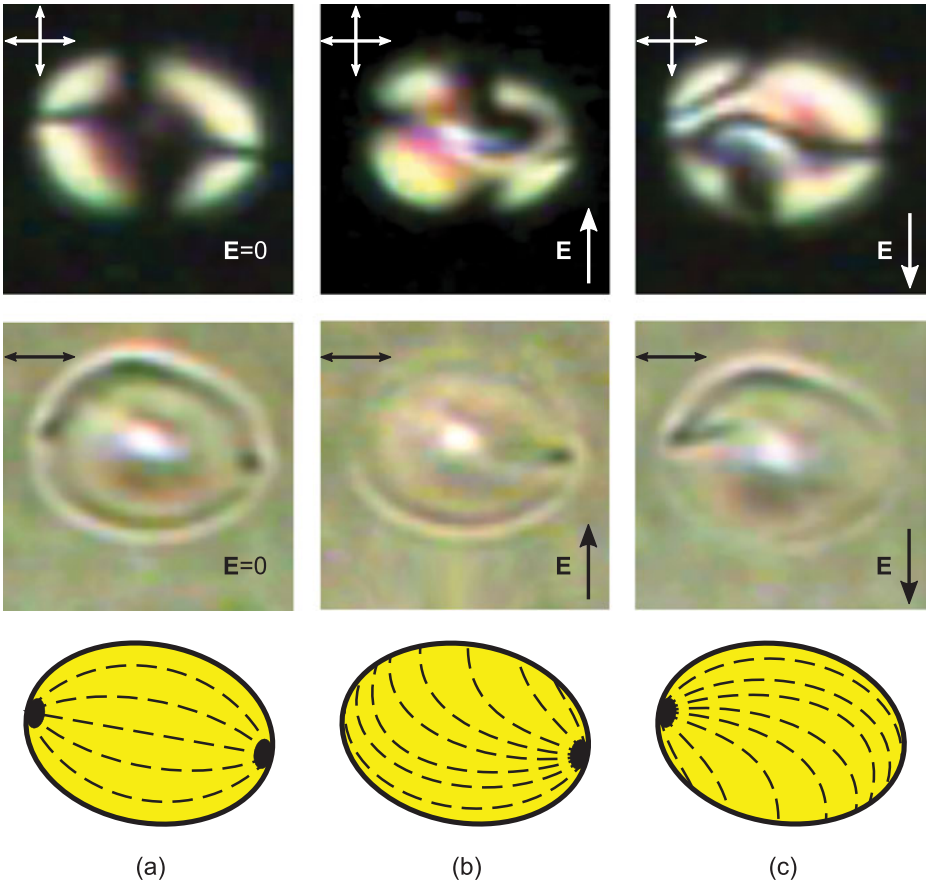

Figure 7.5: The arrangement of pictures and notations are as in Figure 7.4. The electric field $U = 950$ V is directed at an angle of 81° to the droplet's major axis. The field is switched off (a); the electric vector **E** is directed upward (b) and downward (c) in the figure plane. The major axis of the droplet is 15 μm.

Noteworthy is the fact that almost half of the visible droplet boundary is blurred when the field is perpendicular to the bipolar axis (top border in Figure 7.5(b) and bottom one in Figure 7.5(c), middle row). This occurs because the refractive indices of LC and polymer are matched; as a result, the light scattering for this polarization becomes markedly smaller for such LC structure than for the bipolar configuration. This inference is consistent with the results of our measurements of light transmission of PDLC film under direct current (DC) electric field applied perpendicular to the film, which show that the transmittance increased approximately doubles evidencing the promise to use this effect in electro-optical devices.

The possibility that the monopolar structure can appear was analyzed theoretically by the computer simulation of director distribution in a nematic droplet. The LC free energy was minimized in a single-constant approximation (Zumer and Doane, 1986):

$$F = \frac{1}{2}\int K\left[(\nabla\cdot\mathbf{n})^2 + (\nabla\times\mathbf{n})^2\right]\mathrm{d}V \tag{7.1}$$

where a unit vector $\mathbf{n}$ is the nematic director, and K is the averaged value of the basic NLC elastic constants $K = (K_{11} + K_{22} + K_{33})/3$, where K_{ii} (i = 1,2,3) were taken from Bunning et al. (1981). This method was adapted earlier for the calculation of orientational structures in the spherical nematic droplets with inhomogeneous boundary conditions (Prishchepa et al., 2005). We extended this approach for the simulation of nematic droplets shaped as ellipsoid (Prishchepa et al., 2006). As discussed above, the field of spatially separated ions in the droplets compensates the action of the external electric field. For this reason, the terms accounting for the LC energy in the electric field were omitted in eq. (7.1). The boundary conditions were chosen according to the experiment demonstrated in Figure 7.4. Using the data obtained for the director configuration (Figure 7.6, bottom row), the corresponding texture patterns for the crossed polarizers were calculated by the well-known theoretical method (Ondris-Crawford et al., 1991) (Figure 7.6, top row).

One can see that these calculations properly describe the bipolar director configuration and the texture for the prolate nematic droplets (Figure 7.6(a)). To simulate the monopolar structure shown in Figure 7.4(b) and (c), tangential anchoring was assumed for the most part of the droplet surface (~0.7 of the visible boundary; see Figure 7.6(b)). The homeotropic boundary conditions are introduced in a small portion (~0.1 of the boundary on the right). The boundary conditions were assigned to be free between these two areas. The resulting director configuration and the texture pattern (Figure 7.6(b)) agree basically with the experiment (Figure 7.4(b) and (c)), confirming that the above analysis of the experimental data is correct.

The distinctions between the observed effect and other phenomena initiated by ionic impurities in nematic LCs should be discussed. Among these phenomena, various types of electrohydrodynamic instability of nematics in an alternating electric field are well known (Blinov et al., 1984; Fréedericksz and Tsvetkov, 1935). In such

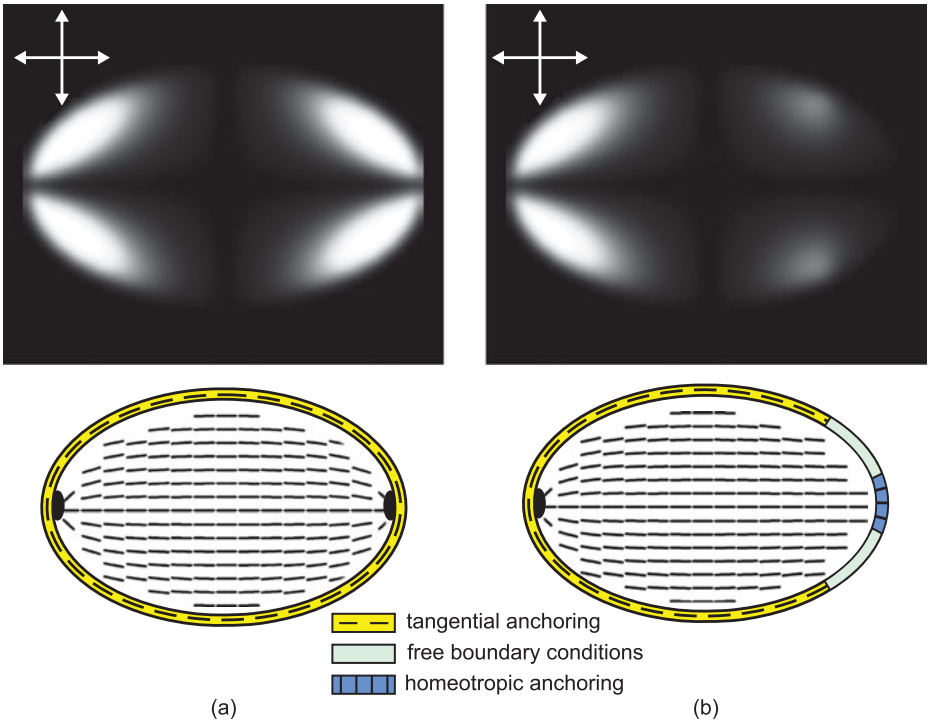

Figure 7.6: Numerical calculation of the director configurations (bottom row) and the corresponding textures (top row) in crossed polarizers for a nematic droplet with the size parameters and boundary conditions close to the experiment (see Figure 7.4). The boundary conditions (tangential, free, and homeotropic) are indicated in the droplet shells (bottom row in the figure). Bipolar orientational structure with the homogeneous tangential anchoring (a). Monopolar structure with the inhomogeneous boundary conditions (b).

systems, the ionic vortex motion initiates corresponding flows in the LC. The initially homogeneous director orientation becomes destroyed and the LC bulk breaks down into a lot of light-scattering vortices.

Another type of phenomena is described in detail by Barbero and Evangelista (2006) and is associated with the selective absorption of ions by the interface in the absence of an external field, as a result of which an electrical double layer forms near the surface. The electric field of the double layer can dominate other orientational actions of the substrate and can govern the director orientation at the LC cell surface.

The electrically induced anchoring transition in LC doped with CTAB is based on the combined action of two properties of the used dopant. The ion-forming ability of the additive makes possible the electrically controlled transport of certain ions to the required area of the LC cell. The surface-active property of the CTA^+ layers formed in this area allows the tangential orientational influence of the PVB matrix

to be screened and the surface anchoring to be changed from tangential to homeotropic. A similar screening effect is described by Blinov et al. (1984) for Langmuir layers formed by molecules of stearic acid. However, the use of electrically neutral molecules does not permit electrically controlled modification of the surface anchoring.

7.2.3 Inverse mode of the electrically induced anchoring transition in nematic droplets

In this section, the possibility of an inverse regime for the ionic modification of surface anchoring is considered and it is shown that this effect can be observed at a higher surfactant concentration than for the above-described case. PDLC films prepared by emulsification of LC in a polymer solution followed by solvent evaporation were studied (Drzaic, 1995). For this purpose, the weight ratio 5CB:PVA:Gl:CTAB of the components was 1:19:6:0.1. Note that the surfactant concentration was 10 times higher than for the normal mode (Zyryanov et al., 2007). It is known that the nematic 5CB is aligned tangentially at the surface of PVA even in the presence of glycerin additions (Drzaic, 1995). The CTA^+ ions, being adsorbed on the interface, can form nanosized layers that specify the homeotropic alignment of the LC molecules at a certain concentration (Cognard, 1982).

The samples of the composite films of 30 μm thickness were placed on a glass substrate with electrodes allowing a DC electric field to be applied along the film plane (Figure 7.7). The size of LC droplets was in the 7–11 μm range. Some of the studied samples were subjected to the uniaxial stretching for the purpose of studying specific features of the structural transformations in prolate droplets. For the material components used, the ordinary refractive index $n_\perp$ of LC is approximately equal to the polymer refractive index n_p. This is convenient for analyzing the director orientation at

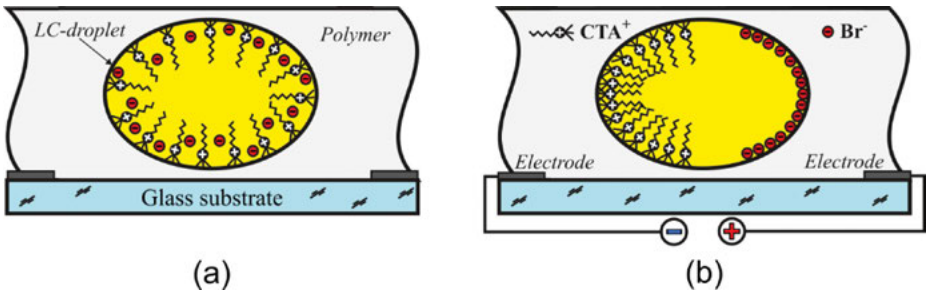

Figure 7.7: Schemes of electrically controlled ionic arrangement at LC droplet boundary for inverse mode. When the electric field is switched off, CTA^+ ions adsorb homogeneously at the interface and specify the homeotropic LC orientation at whole droplet surface (a). Under the action of DC electric field, CTA^+ ions leave a part of the surface close to the anode (b) where the tangential boundary conditions are formed.

the interface between the nematic and polymer. In the case of a switched-off analyzer, the droplet boundary is virtually unseen in the areas where light is polarized perpendicular to LC director. And vice versa, due to the strong light scattering, the interface is clearly seen as a dark line in the areas where the director coincides with the light polarization.

The experiments were accompanied by the numerical calculations of the director configurations in LC droplets and the corresponding textural patterns. The orientational structures were calculated by the well-known method of minimizing the energy of elastic distortions of the director field in the bulk of LC, as discussed above. The droplet shape and the boundary conditions were taken in accordance with the experimental data. The textural patterns of LC droplets in the crossed polarizers were calculated using the theoretical model (Ondris-Crawford et al., 1991).

In all studied samples of the composite films, the radial structure (Figures 7.8–7.10, top row) with the bulk hedgehog defect (Volovik and Lavrentovich, 1983) in the droplet center was initially formed. The typical textural pattern of the droplets in crossed polarizers has a form of Maltese cross. This implies that the used concentration of homeotropic surfactant suffices to form a CTA^+ layer over the entire surface blocking the tangential orienting action of the polymer matrix.

The corresponding schemes of the director distribution in the bulk of the droplets (Figures 7.8(d)–7.10(d), top row, where the central section of the droplet parallel to the film plane is shown) and their textural patterns (Figures 7.8(c)–7.10(c), top row) can be calculated using the condition of the homogeneous homeotropic director alignment over the entire droplet surface. In some droplets, the extinction bands are bent (Figure 7.10(b), top row), indicating that the director lines are twisted. In this case, a small chirality of the nematic structure should be considered in the analysis.

The textural patterns change drastically under the action of an electric field (Figures 7.8–7.10, bottom rows). In this case, the observed transformations can proceed following three various scenarios that ultimately result in the formation of three novel structures, whose specifics are determined by director distribution near the surface in the region with tangential anchoring.

Transition of the radial configuration into the structure containing surface point defect (boojum) and linear ring-shaped surface defect (Figure 7.8). At the beginning of the transformation, a small area with tangential anchoring surrounded by a region with a gradual change of the director orientation from tangential to homeotropic appears on the right side of the droplet surface. A point surface defect (hyperbolic boojum (Meyer, 1972)) is formed at the center of the region with tangential anchoring. Unlike a radial boojum (Volovik and Lavrentovich, 1983), the director lines in this case do not enter this defect and deflect from it along the trajectories close to the hyperbola. Then the region with the tangential director alignment expands, while the hedgehog moves from the droplet center to the hyperbolic boojum and merges with it forming a radial boojum. At the end of the process, the tangential anchoring occupies more than half of the droplet surface. The edges of this region are situated where a

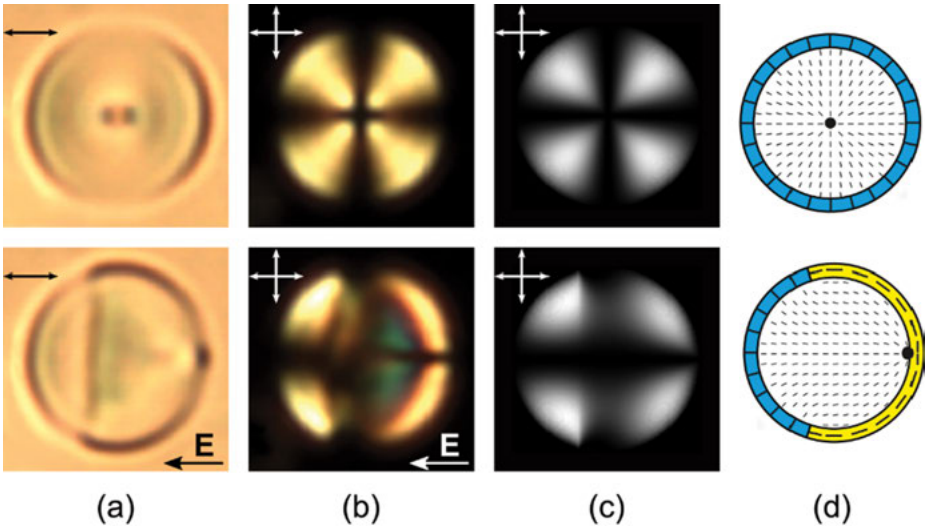

Figure 7.8: Transformation of the radial director configuration (top row) into the structure containing boojum and ring-shaped surface defect (bottom row) under the action of the in-plane applied DC electric field **E**. Photographs of nematic droplets with a switched-off analyzer (a) and in crossed polarizers (b). Calculated director configurations in cross section of the droplet (d) and the corresponding droplet textures in crossed polarizers (c). The boundary conditions (tangential or homeotropic) are indicated in the droplet shells (d). The droplet size is 10 µm.

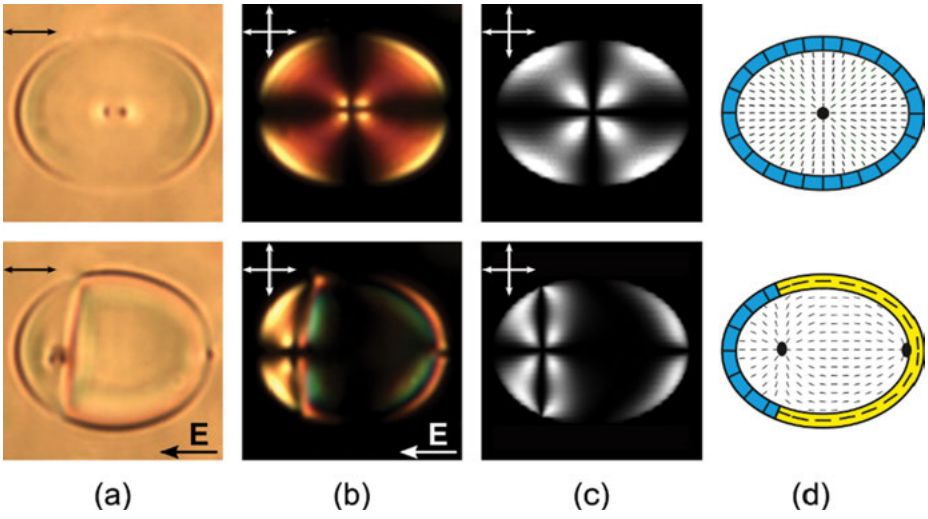

Figure 7.9: Electrically induced transformation of the radial configuration (top row) into the structure containing a hedgehog, boojum, and ring-shaped surface defect (bottom row). Photo positions, simulation data, and notations as in Figure 7.8. The major axis of the droplet is 19 µm.

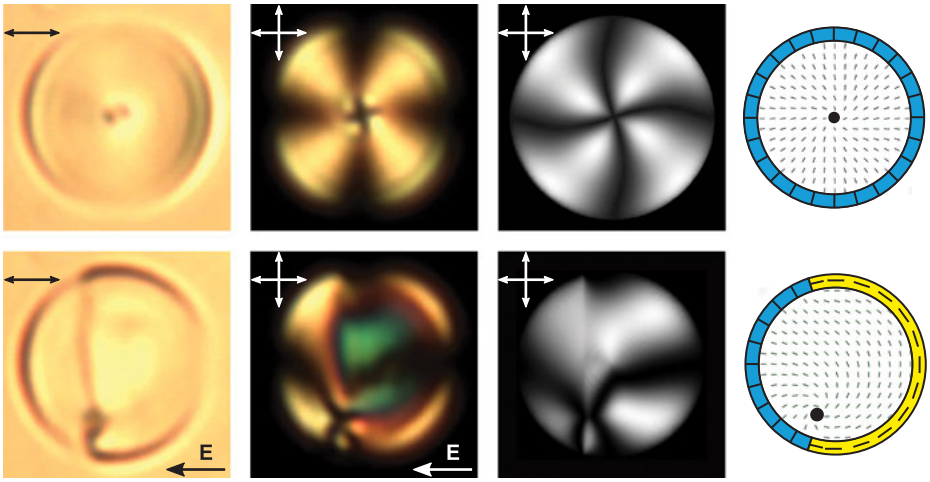

Figure 7.10: Electrically induced transformation of the radial configuration (top row) into the structure containing a hedgehog and ring-shaped surface defect (bottom row). Photo positions, simulation data, and notations as in Figure 7.8. The droplet size is 10 μm.

dark line corresponding to the strong light scattering terminates abruptly at the droplet boundary (Figure 7.8(a), bottom row). Two regions with different director orientations on the polymer wall are separated by a surface defect in the form of a ring perpendicular to the film plane. It is seen in the bottom row of Figure 7.8(a) as a dark vertical line to the left of the droplet center. The structure described in this figure can form in the spherical droplets, although its occurrence is possible in the prolate droplets if the electric field is directed along their minor axis. The resulting director distribution can be modeled using the appropriate boundary conditions (Figure 7.8(d), bottom row). It should be emphasized that, in this case, the director field lines must emerge from the boojum radially in all directions in LC bulk. The droplet texture (Figure 7.8(c), bottom row) obtained using the calculated configuration coincides basically with the experimental pattern (Figure 7.8(b), bottom row), confirming correctness of the analysis.

Transition of the radial configuration into the structure containing a hedgehog, boojum, and surface ring-shaped defect (Figure 7.9). This transformation occurs most frequently in the prolate droplets if the electric field is directed along their major axis. At the beginning of the process, boojum arises on the right side of the surface. Near the boojum, a ring-shaped surface defect forms at the interface between the areas with the tangential and homeotropic anchoring, whereupon it gradually moves to the left half of the droplet. The hedgehog shifts to the plane of the ring-shaped defect. This completes the structural transformation. As shown, the simulation data also describe the experiment well.

Transition of the radial configuration into the structure containing a hedgehog and ring-shaped surface defect (Figure 7.10). This process is observed most frequently in the radial droplets with the originally twisted director lines and proceeds in a qualitatively different way. In this structure, a ring-shaped surface defect also appears at the interface between the tangential and homeotropic anchoring. The hedgehog moves from the droplet center to the plane of the ring-shaped defect and shifts to the surface stopping short of reaching it. Analysis of the photos shows that the defect-free, nearly homogeneous director distribution is formed in the tangential surface zone. In our calculations, we tried to take this fact into account by specifying the director lines at the tangential surface area to be parallel to the line shown in droplet shell (bottom row of Figure 7.10(d)). Although the resulting texture (Figure 7.10(c), bottom row) does not fully coincide with the experimental pattern (Figure 7.10(b), bottom row), the main features (hedgehog position, direction of extinction bands emerging from hedgehog) agree with each other.

All processes described above are reversible. It should be noted that all three variants of the structural transition can occur in the same spherical droplet under the same experimental conditions. The reasons for which one or another transformation scenario is realized call for further investigations. It is likely that the decisive role in these systems is played by the thermal fluctuations producing certain distortions of the radial structure at the instant the electric field is switched on. However, it is shown above that the balance between the probabilities of these processes can be strongly shifted by varying the material parameters or experimental conditions.

A characteristic distinction between the two modes of the electrically controlled ionic modification of the interface is as follows. In the normal regime of the effect (Zyryanov et al., 2007), the initial alignment of the LC is determined by the polymer matrix, while the electric field induces the formation of a layer of surface-active ions in the respective region of the droplet surface, thereby blocking here the orienting effect of the polymer. Zyryanov et al. (2007) mention that the initial tangential LC alignment was changed in a local region of the interface to the homeotropic alignment inherent in the used surfactant. However, the reverse reconstruction of the boundary conditions in a normal mode is also possible, for example, for a composite of homeotropically orienting polymer and ionic surfactant providing the tangential anchoring.

In the inverse regime considered in this section, the initial structure of the LC droplets is governed by the nanosized layer of the surface-active ions, which covers the entire interface because of a high surfactant concentration. Under the action of electric field, ions leave the corresponding surface region, where the boundary conditions characterizing a polymer matrix are formed. By choosing various combinations of the orienting abilities of the polymer and surfactant, one can implement other variants in the reconstruction of the boundary conditions and, respectively, various scenarios of the structural transformations. Moreover, our study has shown that

the resulting director configurations and, hence, the optical properties of the PDLC films are quite sensitive to the material and structural parameters of the medium, such as the surfactant concentration, LC chirality, and droplet anisometry.

7.2.4 Optical response dynamics of polymer-dispersed nematic liquid crystal films

In this section, the electro-optical characteristics of a composite film based on a polymer containing dispersed NLC doped with an ionic surfactant are considered. The polymer matrix of PDLC films was PVA plasticized by glycerin (Gl). The nematic 5CB doped with a cationic surfactant CTAB was encapsulated in the PVA matrix using emulsification technique (Drzaic, 1995b). The ratio of components in the obtained PVA–Gl–5CB–CTAB composition was 9.3:3.7:1:0.02 by weight. The indicated CTAB content was enough to assign normal boundary conditions at LC–polymer interface, so that a radial director configuration was formed inside the NLC droplets in the initial state. These conditions are characteristic of the inverse regime of ion modification of the interface (Zyryanov et al., 2008). The LC droplets had an average diameter of 2–3 μm in plane of the film which had a thickness of about 16 μm. The sample film was formed on a glass substrate with two stripe electrodes spaced by 1 mm. Thus, the field between the electrodes was oriented mainly parallel to the PDLC film. The voltage applied to the electrodes had the shape of rectangular monopolar pulses of variable duration and amplitude.

The electro-optical characteristics of PDLC film were studied using radiation of a Mitsubishi ML101J21-01 semiconductor laser operating at $\lambda = 658$ nm. The laser radiation was sequentially transmitted through the linear polarizer, sample, and diaphragm and then measured by a photodetector. The diameter of the beam cross section was about 0.8 mm. Scattered radiation was blocked by the diaphragm, so that only the straight passing light was detected. The cell with PDLC film was arranged so that the electric field was perpendicular to the laser beam and the light polarization.

NLC droplets in the initial state observed in the geometry of crossed polarizers exhibit structures of the Maltese cross type, which are characteristic of a radial director configuration with a point defect in the droplet center. The structure remains almost unchanged under the action of an applied electric field with a strength of up to 0.03 V/μm. As the field strength is increased further, part of the interface closest to the anode becomes free of CTA^+ surfactant ions and, as a result, tangential boundary conditions (characteristic of the given polymer) are restored in this surface region. For this reason, the configuration of the LC director is transformed so that the fraction of the droplet surface that produces strong scattering of the incident radiation sharply increases (see, for example, Figure 7.8(a), bottom row). These changes in the orientational structure of NLC droplets are clearly manifested in the macroscopic optical response.

Figure 7.11 shows the typical time-evolved waveforms of the optical response of a PDLC film to electric field pulses of various amplitudes. The light transmission T of the film for a normally incident light was 0.77 at small electric field strength up to $E = 0.03$ V/μm. The application of a field with $E = 0.04$ V/μm leads to a decrease in the optical transmission, which can be plainly explained for the employed scheme of measurements by the enhanced light scattering by the NLC droplets with a modified orientational structure. After switching off the field, the transmission is restored to the initial level within a time of approximately 11 s. The dependence of the transmittance change, $\Delta T \propto E$, exhibits saturation at $E = 0.05$ V/μm (Figure 7.11(a)), for which it reaches a level of $\Delta T \propto 0.23$ (Figure 7.12). This value of ΔT is retained as the field strength is increased up to $E = 0.07$ V/μm (Figure 7.11(b)) and decreases with further growth in the field strength.

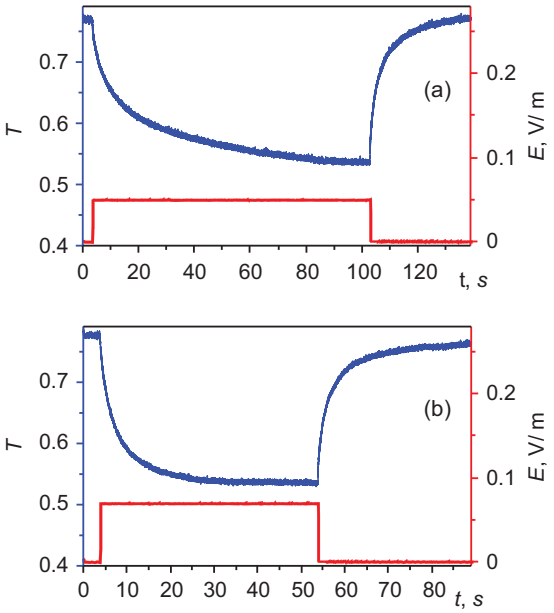

Figure 7.11: Oscillograms of the optical response of a PDLC film to electric field pulses of various amplitudes: $E = 0.05$ V/μm (a) and $E = 0.07$ V/μm (b). T is a light transmission of the PDLC cell.

Analogous variations can be traced for the field dependences of the dynamic parameters of the optical response (Figure 7.12). The response switch-on time τ_{on} decreases to 10 s at $E = 0.07$ V/μm, which is explained by a diffusion character of the ion motion. Indeed, the higher the field strength, the shorter time is sufficient to destroy the screening layer of ionic surfactant at the surface of NLC droplet. However, this tendency is only retained until $E = 0.07$ V/μm. As the field strength increases further, the τ_{on} value begins to increase, exhibits a local maximum at $E = 0.08$ V/μm, and then drops again.

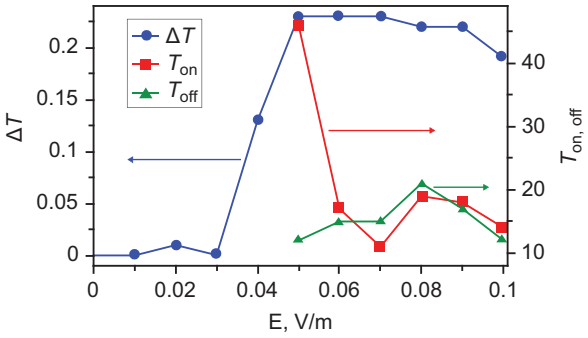

Figure 7.12: Plots of the transmittance modulation ΔT, optical response time (τ_{on}) and relaxation time (τ_{off}) versus applied electric field strength E for the PDLC film.

In contrast, the relaxation process exhibits no such a strong dependence on the applied field amplitude. The relaxation time varies within $\tau_{off} = 10–20$ s. In the range of field amplitudes up to $E = 0.08$ V/μm, this value first somewhat increases and then begins to decrease.

Thus, using the ionic-surfactant method to modify the surface anchoring of NLC droplets in PDLCs, it is possible to transform the orientational structure of LCs and, hence, to control the macroscopic optical characteristics of these composite films. A specific feature of this method is the use of a DC electric field, whose switch-off leads to recovery of the initial LC state. The optical response exhibits a threshold character of its dependence on the applied field strength. In a sample used in this study, the reorientation proceeds rather slowly, with a minimum response and relaxation times of about 10 s. However, as it will be shown later, the response speed may be increased by optimizing the composition, structure of LC material, and experimental conditions. An evident advantage of ionic-surfactant operation (ISO) method is the small strength of the control field, which is three times less compared with that for conventional PDLC films with analogous morphology parameters (Doane, 1991) that operate based on the Frederiks effect.

7.2.5 Bistability in polymer-dispersed cholesteric liquid crystals operated by ionic-surfactant method

In this section, a memory effect is considered which is caused by the ionic modification of the surface anchoring under the action of electric field in the polymer-dispersed ChLC (PDChLC) films.

Lately, technologies aimed at reducing the energy consumed by LC devices have been developing extensively. One of the effective solutions to this problem can be based on the use of a bistability phenomenon that allows a preset optical state to be

retained in the absence of an electric field. In this respect, much attention is devoted to ChLCs in which the bistable optical states of various types can be realized (Berreman and Heffner, 1981; Crawford and Zumer, 1996; Grawford, 2005; Greubel, 1974; Hsu et al., 2004; Yang, 2006; Yang et al., 1997). A most widely used effect that is already employed in display devices consists in switching a ChLC between stable states with a planar structure and a focal conic domain structure (Crawford and Zumer, 1996; Yang, 2006; Yang et al., 1997). The cholesteric helix pitch P must be much smaller than the size D of a cavity filled with the LC. The planar structure of a ChLC selectively reflects the circularly polarized light component, while the domain structure intensively scatters all radiation. If a ChLC is put onto a light absorbing substrate, the cell would reflect the light at a certain wavelength in one state and appear black in the other state. This effect is operative in both planar ChLC layers and ChLC droplets dispersed in a polymer film (Crawford and Zumer, 1996; Yang et al., 1997). The latter case is of special interest, since it enables the development of flexible bistable reflective displays (Yang, 2006), although the small pitch of the cholesteric helix makes necessary large control voltages. The memory effect is also characteristic of PDChLC films with a helicoid pitch comparable to the diameter of ChLC droplets ($P \cong D$) (Zyryanov et al., 1994), but the retention of recorded information in this case requires a supporting voltage (Barannik et al., 2005).

The aim of this study was to assess the alternative possibility of using PDChLC films in bistable optoelectronic devices and displays with nonvolatile data storage. The samples of PDChLC films were prepared by the emulsification of a ChLC in an aqueous solution of PVA plasticized by glycerin (Gl), followed by the evaporation of solvent (Drzaic, 1995; Klingbiel et al., 1974). The ChLC was a mixture of nematic LC 5CB with 1.5 wt% of ChA. The cationic surfactant CTAB was dissolved in the ChLC mixture before the preparation of emulsion. The ratio of components in the obtained ChLC–PVA–Gl–CTAB composition was 1:19:6:0.1 (w/w). At this concentration, CTA^+ ions adsorbed on a polymer surface form a layer that changes the surface anchoring from tangential to homeotropic (Zyryanov et al., 2008b).

The photographs in Figures 7.13–7.15 show the fragments of PDChLC films in various states as observed in crossed polarizers. PDChLC film was confined between two glass plates with transparent ITO electrodes. This sandwich structure was arranged between crossed polarizers, and an AC electric signal of rectangular or sinusoidal shape was applied to the electrodes. The radiation of a semiconductor laser operating at $\lambda = 658$ nm was transmitted through the optical cell and detected by photodiode, and the output signal of which was analyzed using a digital oscilloscope.

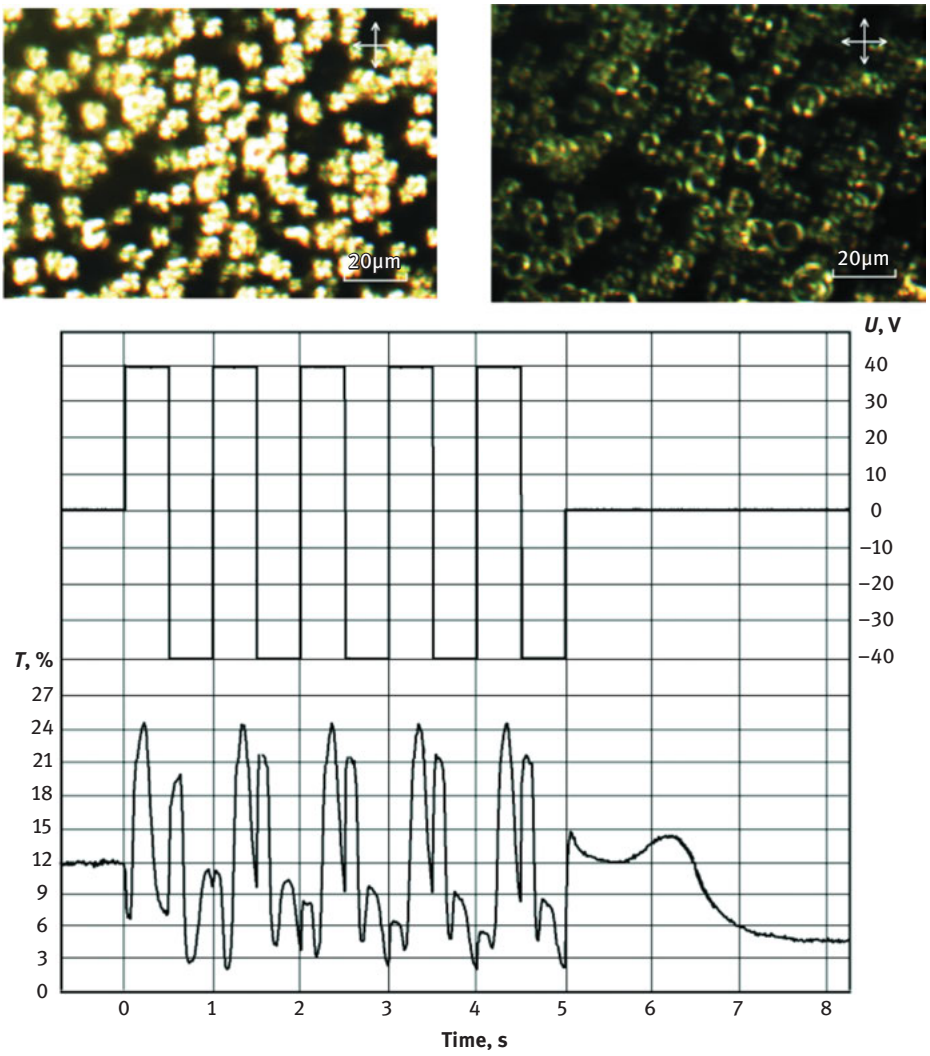

Figure 7.13: Waveforms of applied electric voltage *U* (top) and optical transmittance of a PDChLC film switched from the initial state with a twisted radial structure into a stable intermediate state (bottom). Photographs of film fragment in equilibrium states before (top row, left) and after (top row, right) electric field application. Here and below, the photographs are taken in crossed polarizers oriented parallel to picture sides.

The PDChLC film thickness was 75 μm. The ChLC droplets in the film plane had round shapes with an average diameter of 9 μm. These droplets were arranged in the film without overlap, which allowed the orientational structure of ChLC to be identified. In ChLC droplets without a surfactant, a twisted bipolar configuration of the LC director was formed, which correspond to a tangential anchoring. ChLC droplets

containing about 10% CTAB exhibited a twisted radial structure corresponding to a homeotropic orientation of LC molecules on the surface of the polymer matrix. The optical textures of these droplets in crossed polarizers resemble a bent Maltese cross (Figure 7.13, top row, left). Since the droplet transmits only a fraction of the incident light, while the optically isotropic polymer matrix does not transmit light in crossed polarizers, the total optical transmittance of a PDChLC film in the initial state amounts to only about 12% (Figure 7.13).

Under the action of an applied electric field, the ChLC droplets can transform into either the stable state with a homogeneous orientation of the director perpendicular to the film plane or into some intermediate stable structures. In the former case, the birefringence of the ChLC does not manifest and the light is not transmitted through these droplets (Figure 7.14, top row, right). Note that a small fraction of droplets (not exceeding 2% for the sample studied) does not transform into a homogeneous state, which accounts for a weak residual transmittance (Figure 7.14, top row, right). In the intermediate states, the LC director in the central part is close to the normal to the film surface and is tilted in the equatorial region. For this reason, the light only passes through the side regions (adjacent to the visible boundaries) of droplets (Figure 7.13, top row, right).

Thus, the optical transmittance of the PDChLC film in stable states can vary within 1.5–12%. From the initial state with $T = 12\%$, the PDChLC film can be switched to stable intermediate states by applying rectangular electrical signal at a frequency of 1 Hz (Figure 7.13). Under the action of this AC field, ChLC droplets exhibit a complicated process of transformation of the orientational structure, which involves the contributions of various physical phenomena including the Frederiks effect, modification of boundary conditions, and electrohydrodynamic instability related to the ion transport. The reorientation of the droplets manifests in the form of optical response, which varies during the electric signal within $T = 2.0–24.5\%$. After switching off, the droplets relax within about 3 s to an equilibrium intermediate state. The resulting transmittance can be controlled by varying the number, amplitude, and duration of pulses.

The minimum optical transmittance in a stable intermediate state achieved for the given samples controlled by rectangular pulses was about 4.5–5%. This value can be further reduced to 1.5%, but this requires applying a 1.3 kHz sinusoidal signal for 2 s after the rectangular pulses (Figure 7.14). This additional action leads to a homogeneous orientation of the LC director in droplets and the resulting almost complete darkening of the optical picture (Figure 7.14, top row, right). After this transition to a homogeneous orientation, only a small fraction of droplets (about 1%) can relax over time (for the first 100 h) to an intermediate structure, after which the system is completely stabilized.

Both intermediate and homogeneous structures of ChLC droplets can be returned to the initial state by applying rectangular voltage pulses with a frequency of 2 Hz, for example, to return droplets into the initial state with a twisted radial configuration of the director and the corresponding optical transmittance, it is possible

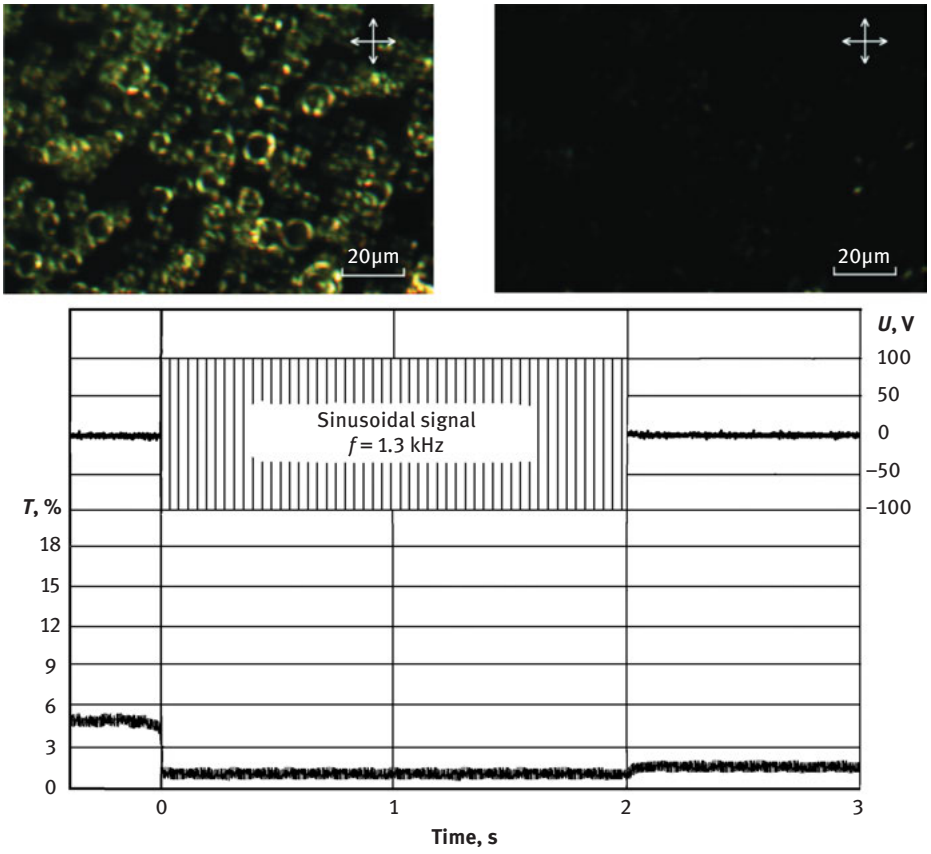

Figure 7.14: Waveforms of the control sinusoidal electric voltage *U* (top) and optical response of a PDChLC film switched from an intermediate state into a stable state with homogeneous LC director orientation in the droplets (bottom). Photographs of the film fragment in an intermediate state (top row, left) and in a stable state with homogeneous director orientation perpendicular to the film plane (top row, right).

to use the sequence of signals shown in Figure 7.15, with a gradually decreased (from 40 to 25 V) amplitude.

Thus, using ionic surfactants that modify the boundary conditions under the action of an applied electric field, it is possible to obtain many stable structural and optical states of a PDChLC film containing weakly twisted ChLC (i.e., with helicoid pitch comparable to the droplet size). This film material has good prospects for the development of electro-optical devices that do not require a fast response (electronic books, optical shutters, smart windows, etc.), but ensuring nonvolatile conservation of recorded information or a preset level of optical transmittance. Additional advantages of the proposed material are related to its flexibility, mechanical strength, and simple manufacturing technology.

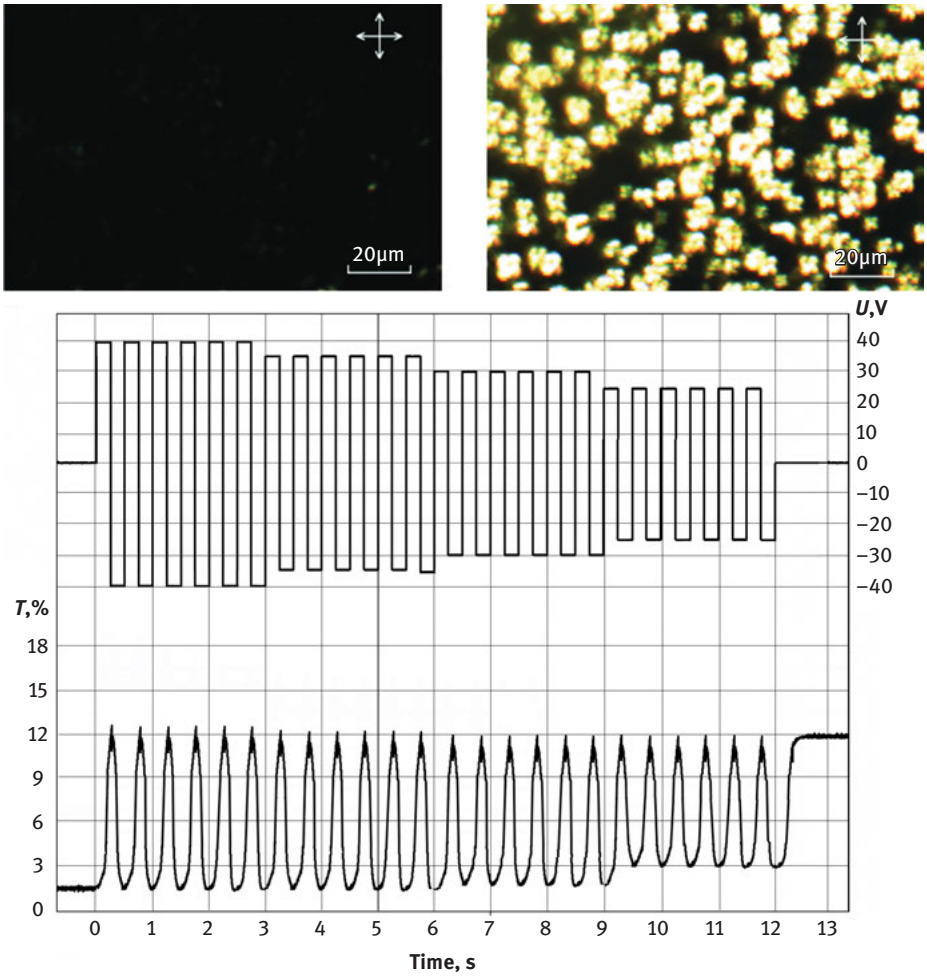

Figure 7.15: Waveforms of control electric voltage *U* (top) and optical response of a PDChLC film switched from a state with homogeneous LC director orientation into the initial state with a twist radial structure in the droplets (bottom). Photographs of the film fragment in a state with homogeneous director orientation perpendicular to the film plane (top row, left) and in a state with a twist radial structure in the droplets (top row, right).

The list of LC structures to which the ISO method can be applied is not restricted by the PDLC materials. These can be various LC structures in which the role of the substrate or matrix is performed by solid media, polymers, liquids, and others.

7.3 Liquid crystal layers controlled by ionic-surfactant method

7.3.1 Ionic-surfactant-doped nematic layer with homeotropic–homeoplanar configuration transition

LC cells consisting of two glass substrates with transparent ITO electrodes on the inner sides and a nematic layer between them can also be controlled by the ISO method. The nematic LC 5CB doped with CTAB was used in the experiments. Polymer films with a thickness of about 1.5 μm were preliminarily deposited on the electrodes. These films serve simultaneously as an orienting coating and a protective layer preventing the contact of surfactant ions with the electrodes. Polymer films based on PVA and glycerin solved in water were formed by the method of spin coating of the solution with subsequent drying. It is known that such films specify planar boundary conditions for the nematic 5CB (Cognard, J. 1982). The easy orientation axis was formed by the mechanical rubbing of the polymer surface in a required direction. The cells were filled with the LC by the capillary method in the isotropic phase. The thickness of the LC layer in the samples under study was about 6 μm.

The optical textures of nematic layer were studied by POM Axio Imager A1 (Carl Zeiss), which allows taking the photo and video recording of proceeding processes. The observations and measurements were carried out in the crossed polarizer geometry. Rectangular monopolar pulses of the electric field from an AHP 3122 (AKTAKOM) generator were applied to the ITO electrodes. To study the dynamics of the macroscopic optical response of LC cell, we used a He–Ne laser (Linos) with a wavelength of $\lambda = 633$ nm. The laser radiation passed successively through the polarizer, an LC cell, and an analyzer and arrived at a photoreceiver. The diameter of the cross section of the laser beam was 1 mm. The angle between the direction of the rubbing of the substrates and the direction of polarizers was 45°.

Figure 7.16 shows the scheme for implementing the effect of the electrically controlled modification of the surface anchoring. It is necessary to choose the concentration of CTAB in 5CB such that the nanolayer of CTA^+ cations adsorbed at the interface can screen the planar orienting action of the polymer film and specify the homeotropic surface anchoring (inverse ISO mode). In this case, the homogeneous ordering of the director oriented perpendicularly to the substrates appears in the entire nematic layer in the initial state (see Figure 7.16(a)). When a static electric field is applied, surfactant ions move toward the corresponding electrode and one of the substrates becomes free of the layer of CTA^+ surface-active cations. As a result, planar anchoring conditions characteristic of a polymer coating are formed on this substrate (Figure 7.16(b)). Finally, the orientational transition from the homeotropic structure to the hybrid homeoplanar configuration of the director occurs in the LC cell.

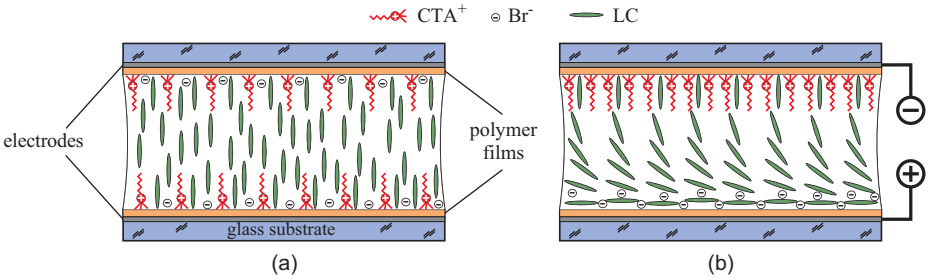

Figure 7.16: Scheme for implementing the effect of the ionic modification of the surface anchoring in the nematic layer. Electric field is switched off; the number of CTA^+ ions adsorbed at the interface is sufficient for the formation of homeotropic anchoring on the top and bottom substrates (a). Bottom substrate under DC electric field becomes free of CTA^+ ions; the orienting polymer film on this substrate specifies the planar ordering of the liquid crystal (b).

The experimental conditions necessary for implementing the schemes described above can be ensured with the use of polymer coatings with the weight ratio of components PVA:Gl = 1:0.243 and nematic 5CB doped with the ionic surfactant in the ratio of 5CB:CTAB = 1:0.01. The photographs of the optical textures of the LC cell are shown in Figure 7.17, where the electrically controlled switching of surface anchoring is demonstrated. One of the substrates (bottom) was preliminarily rubbed, whereas the other substrate (top) was used without rubbing. In the initial state, light does not pass through the optical system irrespective of its azimuthal rotation in crossed polarizers (see Figure 7.17(a)). This indicates the homeotropic orientation of the director throughout the entire nematic layer. When a DC electric field directed from bottom to top is applied (Figure 7.17(b)), the homogeneous bright pattern of LC layer is observed in the steady-state regime. This means that the homogeneous planar ordering of the director oriented along the rubbing direction **R** over the entire area is formed on the bottom substrate. When the polarity of the electric signal is changed, the transmittance

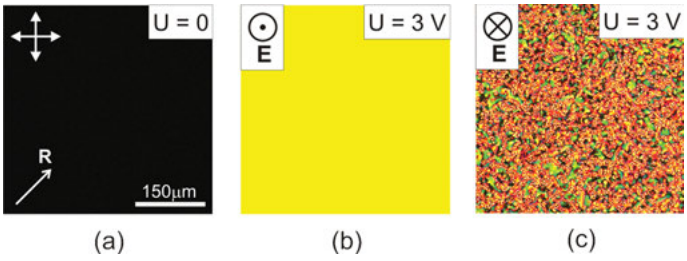

Figure 7.17: POM images of the optical textures of the liquid crystal layer in the initial state (a) and under the DC electric field **E** (b, c) directed from the bottom substrate to the top one (b) and from the top substrate to the bottom one (c). The value of applied DC voltage is $U = 3$ V. The bottom substrate was rubbed in the direction **R** at an angle 45° to the polarizers. The top substrate was not rubbed.

is high, but the optical pattern becomes sharply inhomogeneous (Figure 7.17(c)). This is explained by the absence of an azimuthally preferable direction (easy orientation axis) on the unrubbed substrate with planar anchoring.

These changes of the transmittance of LC cell cannot be attributed to the classical Frederiks effect (Freedericksz and Zolina, 1933) because the nematic 5CB with $\Delta\varepsilon > 0$ was used in the experiment. In the case of this effect, the application of the external electric field perpendicular to the plane of the LC layer would lead to the stabilization of the initial homeotropic orientation of the director. Thus, these observations convincingly demonstrate the anchoring transition in the planar nematic layer, which is due to the switching of surface anchoring from homeotropic to planar on the substrate with the anode electrode.

Figure 7.18 shows photographs demonstrating the optical textures of the LC layer for various control field strengths. In this case, both substrates were rubbed and put so that their rubbing directions were antiparallel. The reorientation process caused by the ionic-surfactant modification of surface anchoring is of a threshold character. The reorientation process begins with the field strength $U = 2.8$ V. The threshold character is due to the existence of the critical density of the layer of adsorbed CTA^+ ions below which the orienting action of the polymer coating is no longer screened. When the critical surface density is reached at certain electric field strength, the modification of surface anchoring begins. The anchoring transition is observed in the pure form in the range $2.8\ \text{V} < U < 3.5\ \text{V}$ (Figure 7.18(b) and (c)). At $U = 3.6$ V, the formation of the texture pattern of domains mainly elongated perpendicular to the rubbing directions begins in the LC layer. These domains are clearly seen at $U = 4.0$ V (Figure 7.18(d)). The formation of domains can be attributed to various surface phenomena (Proust and Ter Minassian Saraga, 1972), and the analysis of which is beyond the scope of this work.

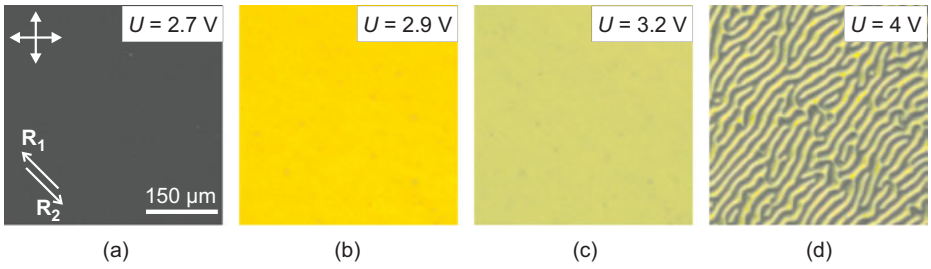

Figure 7.18: POM images of the optical textures of the 5CB layer doped with the ionic surfactant taken under DC voltages $U = 2.7$ V (a), 2.9 V (b), 3.2 V (c), and 4.0 V (d). The notation is the same as in Figure 7.17; $\mathbf{R}_1$ and $\mathbf{R}_2$ are the rubbing directions of the top and bottom substrates, respectively.

The texture patterns considered above correspond to the equilibrium state of modified boundary conditions under DC voltage. However, the most interesting features

of the effect under study are manifested in the response dynamics of LC layer near of the leading and trailing edges of the rectangular electric pulse (Figure 7.19). The pulse duration was 10 s. The transmittance of the cell in the crossed polarizer for the homeotropic LC orientation in initial state (Figure 7.18(a)) is close to zero. Any deviation of the director from the normal always leads to an increase in transmittance.

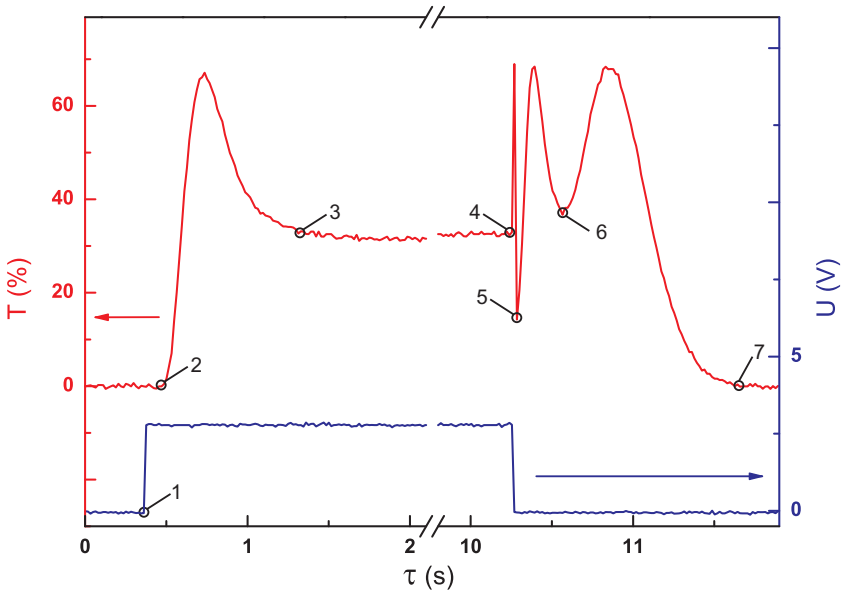

Figure 7.19: Optical response of an LC cell to the pulse of an electric field of 2.8 V. Numbers at transmittance *T* and voltage *U* curves mark the limits of the characteristic time intervals.

The complicated curve of the optical response can be divided into a sequence of time intervals in each of which a certain physical effect dominates. First, a noticeable delay of the optical response with respect to the forward edge of the electric pulse is noteworthy ($\tau_{12} = 0.14$ s, where the subscript "12" indicates two points in Figure 7.19 and the interval between which is considered). This delay appears because ions cannot instantly block the action of switched-on external electric field $\mathbf{E}_0$ in the bulk of the LC. Therefore, in this interval, the classical Frederiks effect occurs stabilizing homeotropic orientation of the nematic with $\Delta\varepsilon > 0$, and the transmittance remains zero. The time of separation of the ion cloud can be approximately taken as the time of the ions passage through the LC layer (Blinov and Chigrinov, 1993):

$$\tau_T = \frac{d^2}{U_{\mathrm{LC}} \cdot \mu} \tag{7.2}$$

where d is the thickness of the LC layer, U_{LC} is the voltage applied to the layer, and μ is the mobility of ions. Using the values $\mu = 10^{-6}$ cm$^2 \cdot$ s$^{-1} \cdot$ V^{-1} (Blinov and Chigrinov, 1993b), $U_{LC} = 1.4$ V (obtained taking into account the presence of polymer coatings), and $d = 6$ μm, we obtain the estimate $\tau_T = 0.26$ s, which is an upper limit for the possible action of the classical Frederiks effect. In reality, it is switched off faster when the effective field $\mathbf{E}_{eff} = \mathbf{E}_0 + \mathbf{E}_i$ (where $\mathbf{E}_i$ is the electric field of the separated ions) decreases below the threshold value of the Frederiks transition. Indeed, the delay time τ_{12} is noticeably shorter than the transit time τ_T.

At time instant 2, the external electric field $\mathbf{E}_0$ is mainly compensated by the field of ions $\mathbf{E}_i$. The planar orienting coating free of CTA^+ cations on one of the substrates begins to turn the director of the LC leading to an increase in transmittance. The T curve reaches a maximum of about 68%, then decreases to 33%, and is finally saturated. This behavior of transmittance can be predicted using the known relation (Born and Wolf, 1999) for an anisotropic plate in crossed polarizers. With the parameters of our experiment, it can be written in the simplified form as follows:

$$T = \sin^2\left(\frac{\pi \int_0^d \Delta n(z)\mathrm{d}z}{\lambda}\right) \tag{7.3}$$

The numerator is the integral optical path difference for the ordinary and extraordinary beams on the thickness of the LC layer and λ is the wavelength of laser radiation. For the homeotropic nematic layer, the integral is in eq. (7.3) and, hence, the transmittance is zero. For the homeoplanar layer of LC 5CB ($n_{||} = 1.7057$, $n_{\perp} = 1.5281$ at $t = 25$ °C and $\lambda = 0.633$ μm (Bunning et al., 1986)) with a thickness $d = 6$ μm, this integral gives 0.511 μm in the approximation of a linear change of director slope over the thickness of the layer. This means that, when the orientational structure of LC varies smoothly from the homeotropic structure into the homeoplanar one, the transmittance increases to a maximum at an integral value of 0.317 μm and then decreases to $T = 32\%$, corresponding to an integral value of 0.511 μm. This behavior of transmittance is in good agreement with the experiment. It confirms the formation of the homeoplanar structure in the electric field.

The time of reaching the steady-state regime $\tau_{23} = 0.75$ s is in essence the time of the switching of surface anchoring plus the relaxation time of the homeotropic configuration in LC bulk into the homeoplanar structure (Figure 7.20(a)). The relaxation processes in LC are described by the formula (Blinov and Chigrinov, 1993)

$$\tau_{rel} = \frac{\gamma \cdot d^2}{\pi^2 \cdot K} \tag{7.4}$$

where γ is the rotational viscosity of LC and K is the corresponding elasticity modulus. Taking the average value $K = 6.3$ pN (Cui and Kelly, 1999b) and $\gamma = 0.09$ Pa·s (Skarp et al., 1980b) for the 5CB LC, we obtain $\tau_{rel} = 0.05$ s. The τ_{23} value is larger

than τ_{rel} by a factor of 15 apparently because of the total effect of two orientational processes indicated above.

The transmittance curve behavior after the switching off electric pulse is even more complicated. In this case, LC layer at the beginning is subjected to the field of separated ions $E_i = E_0$. The classical Frederiks effect again occurs and is manifested in the reorientation of most of LC bulk along the field except for a thin layer near the lower substrate (Figure 7.20(b)). In the time interval $\tau_{45} = 0.02$ s, the transmittance undergoes the inverse evolution, first increasing to the same value of 68% and, then, decreasing to 14%. The complete quenching is impossible because of the presence of the above-mentioned surface region, where a certain phase mismatching of the beams is collected. The switch-on time of the classical Frederiks effect is given by the formula (Blinov and Chigrinov, 1993)

$$\tau_{on} = \frac{\gamma \cdot d^2}{\varepsilon_0 \cdot \Delta\varepsilon \cdot E^2 \cdot d^2 - \pi^2 \cdot K} \tag{7.5}$$

where $\Delta\varepsilon$ is the dielectric anisotropy of the nematic and E is the electric field strength acting on LC. Taking the above γ, d, and K values, as well as $\Delta\varepsilon = 11.2$ (Chandrasekhar, 1977b) and $E = 0.23 \times 10^6$ V/m, which were calculated considering the polymer coatings, we obtain $\tau_{on} = 0.03$ s. This estimate exceeds τ_{45} because the reorientation of LC by the field of ions in experiment remains incomplete. After the external field is switched off, two clouds of separated ions move toward each other. This leads both to a decrease in the LC layer between them, which is subjected to the field E_i, and to a gradual decrease in the field to zero. At the same time, the nematic layer adjacent to the electrode from which bromide anions leave grows rapidly. The recovery of the homeoplanar structure begins here. This process becomes dominant at time instant 5 and lasts at $\tau_{56} = 0.3$ s. This reorientation is in essence like a local transition in interval τ_{23}.

The process begins to complete at time instant 6; when surface-active CTA^+ ions approach, owing to diffusion, the substrate with the planar orienting coatings (Figure 7.20(c)). They are adsorbed on this substrate and begin to form the homeotropically orienting layer, returning the orientational structure of LC to the initial state (Figure 7.20(d)). In this case, the character of a transmittance change becomes opposite. For this reason, the shape of the curve section in the interval τ_{67} is an almost specular reflection of the interval τ_{56} at point 6, but is extended in time to the value $\tau_{67} = 0.95$ s.

Hence, compared with the classical Frederiks effect, where oscillations of the optical response to the leading and trailing edges of the rectangular electric pulse coincide in the number of extrema (Blinov and Chigrinov, 1993b), anchoring transition leads to a more complicated behavior of transmittance (Sutormin et al., 2012).

In addition, we considered the applied voltage dependences of the optical response dynamics of LC cell under study. Figure 7.21 shows the control electric pulses and optical response for several field values. Without an electric field, the transmittance of the cell is close to zero, and transmittance remains invariable as the control

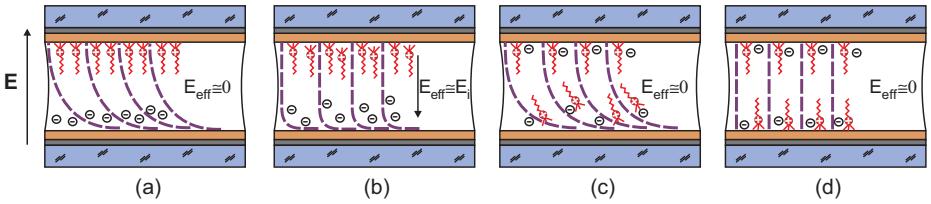

Figure 7.20: Distributions of the director and surfactant ions in the liquid crystal layer at time instants marked by the following numbers in Figure 7.19: (a) 4, (b) 5, (c) 6, and (d) 7.

voltage increases up to $U = 2.5$ V. When $U = 2.6$ V is attained, the variation in the transmittance of LC cell is observed: it reaches the maximum of 67% and then decreases to 29% by the time of the end of the electric pulse (Figure 7.21(a)). This variation is explained by the transition of the director from the homeotropic orientation into the hybrid (homeoplanar) one due to the ionic modification of the surface anchoring. An increase in the control field leads to gradual growth of the transmittance at the electric pulse finish to 64% at $U = 3.1$ V (Figure 7.21(b) and (c)). However, with further increase in the voltage, T gradually drops to 50% (Figure 7.21(d)). The physical mechanisms underlying the specific behavior of the curve $T(\tau)$ during the action of an electric pulse and after its switching off were described in detail above.

Figure 7.22 presents voltage dependences of the dynamic parameters of the optical response. Let us consider the first delay time τ_{del} determined as the time interval between the electric pulse switching on and the start of the transmittance variation (Figure 7.21(a)). As the pulse amplitude grows from 2.6 to 3.3 V, delay time τ_{del} drops from 1.6 to 0.1 s (Figure 7.22(a)). In contrast to the voltage dependence of τ_{del}, the dependence of the on-time τ_{on} determined as the interval between the electric pulse start and transmittance saturation (Figure 7.21(d)) is non-monotonic (Figure 7.22(b)). The value of τ_{on} rapidly decreases from 4.8 to 0.8 s in the voltage range 2.6–2.8 V. This drop in τ_{on} is caused by the acceleration of the modification of the surface anchoring on the substrate with the anode. However, at $U = 2.9$ V, τ_{on} jumps from 0.8 to 3.4 s, and then the on-time smoothly decreases again to 2.1 s at $U = 3.3$ V. It should be noted that an analogous anomaly was observed above in PDLC film controlled by the ionic-surfactant method (Krakhalev et al., 2011). In the range 2.6–2.8 V, τ_{off} grows from 0.3 to 1.1 s and then remains almost invariable up to 3.3 V (Figure 7.22(a)). Such a behavior is typical of many relaxation processes occurring, in particular, in LC cells with the classical Frederiks transition (Blinov, 2011).

The anchoring transitions in LC layers are very sensitive to the concentration and composition of the components. A key role of the protective layer should be noted, which prevents the direct arrival of surfactant ions at the ITO electrodes. In the absence of this layer in our experiments, as well as in Petrov and Durand (1994), electrohydrodynamic instability dominated in the transformation of the LC structure and prevented the observation of the modification of boundary conditions.

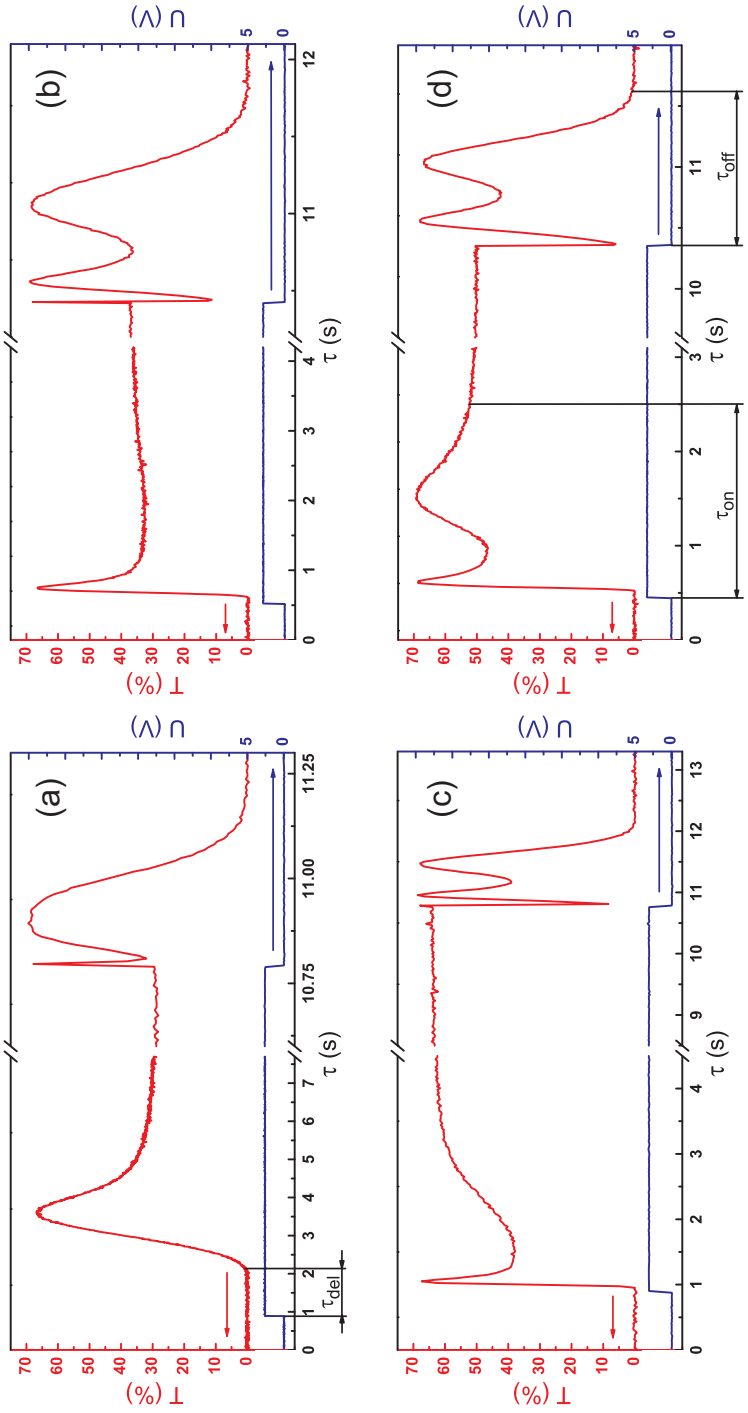

Figure 7.21: Dynamics of the optical response of LC cell controlled by ionic-surfactant method. The amplitude of applied voltage $U = 2.6$ V (a), 2.9 V (b), 3.1 V (c), and 3.3 V (d). The LC layer thickness is 6 µm.

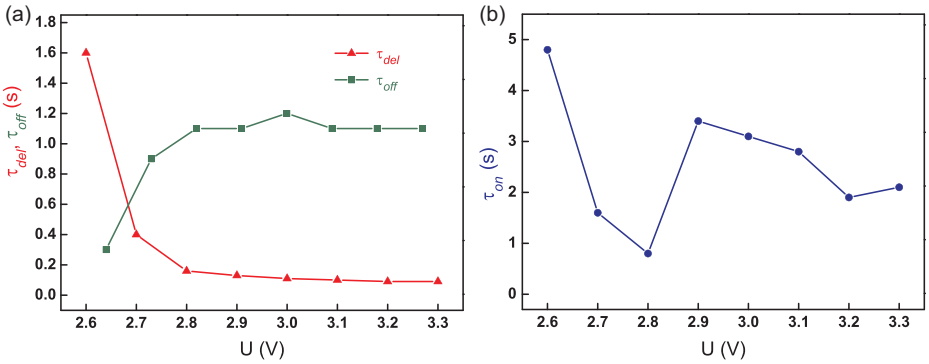

Figure 7.22: Control voltage dependences of delay time τ_{del} (a), relaxation time τ_{off} (a) and on-time τ_{on} (b) of LC cell.

7.3.2 Electrically induced anchoring transition in nematics with small or zero dielectric anisotropy

These experiments were carried out with sandwich-like cells (Figure 7.16). The rubbed polymer films based on the PVA doped with Gl in the weight ratio PVA:Gl = 1:0.29 were used as orienting coatings. The utilized LC materials were the nematic LC MBBA with $\Delta\varepsilon = -0.54$ at 25 °C and the MBBA–5CB mixture in the weight ratio 1:0.02, respectively. The MBBA–5CB mixture had the zero dielectric anisotropy. The nematics were preliminarily doped with ionic-surfactant CTAB in the weight ratio LC:CTAB = 1:0.008.

Since the main factor influencing the anchoring transition is the displacement of the surface-active ions, the same variant of the director reorientation can be realized for the different LCs independently of the sign and value of their dielectric anisotropy (Figure 7.16). For instance, the transition from the homeotropic director configuration to the homeoplanar one caused by the ionic modification of surface anchoring begins at $U = 2.7$ V for the cell based on MBBA ($\Delta\varepsilon < 0$) doped with CTAB. This value is close to the threshold voltage ($U_{th} = 2.8$ V) of 5CB cell operated by the ionic-surfactant method. The reorientation of MBBA cannot be explained by the Frederiks effect since the threshold field would be about 4 V for our cell. The reorientation of LC director is not accompanied by the electrohydrodynamic instability in the range of the control voltage $2.7\ \text{V} \le U \le 4$ V. The domain structure was formed only at the voltage $U \ge 4.1$ V. The on/off time of the MBBA cell under the action of rectangular electric pulse is tens of seconds and exceeds the same parameters for the 5CB cell ($\propto$1 s).

It should be emphasized that the analogous transformation of the orientational structure (Figure 7.16) occurs for the nematic with zero dielectric anisotropy. In the inserts of Figure 7.23, we demonstrate the change in the optical texture of the LC

cell based on the MBBA–5CB mixture ($\Delta\varepsilon = 0$) doped with CTAB and placed between the crossed polarizers under the action of DC electric field. In the initial state, the optical texture of the LC layer is a uniform dark area (left insert of Figure 7.23). The DC electric field induces the modification of the surface anchoring which results in the formation of the hybrid LC structure. This transition leads to the increase of the light transmission of the system (right insert of Figure 7.23). As for other LCs, the reorientation in the cell filled with MBBA–5CB mixture ($\Delta\varepsilon = 0$) exhibits a threshold character starting from 3 V which is approximately equal to the threshold voltages of 5CB cell and MBBA cell operated by the ionic-surfactant method. At the control voltage 3.0 V ≤ U ≤ 4.1 V, the optical texture of LC layer is a uniform light area without a domain structure which begins to form at U > 4.1 V. Thus, the ionic-surfactant method provides an opportunity of the electrically controlled director reorientation of LC with zero dielectric anisotropy.

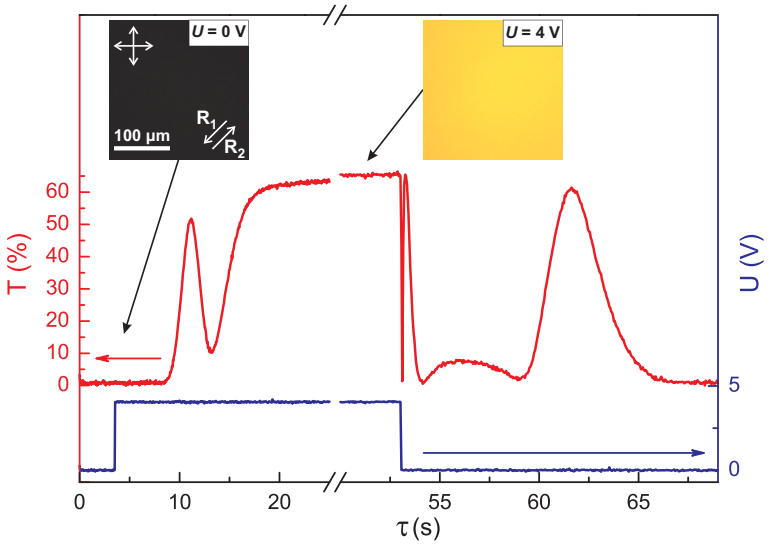

Figure 7.23: Optical response of LC cell based on the MBBA–5CB mixture ($\Delta\varepsilon = 0$) doped with CTAB (the top curve) and electric 4 V pulse (the bottom curve). The inserts show optical textures of LC cell in the initial state (left insert) and under the DC electric field 4 V (right insert). $\mathbf{R}_1$ and $\mathbf{R}_2$ are rubbing directions of the top and bottom substrates, respectively.

7.3.3 Ionic-surfactant-doped nematic layer with homeoplanar–twisted configuration transition

In this section, the transition from the homeoplanar orientational structure to the twisted one induced by the ionic modification of surface anchoring is considered. Such orientational transition leads to a decrease in switching times of LC cell with

ISO. LC cell under study was comprised of two glass substrates with ITO electrodes covered by different polymer films and nematic layer between them (Figure 7.24). The bottom substrate was coated with PVA, while the film of PVA doped with glycerin compound (Gl) in the weight ratio 1:0.432 was deposited at the top substrate. The polymer films were formed using a spin coating technique and then were rubbed. The rubbing directions of polymer films at both substrates were mutually perpendicular. The cell gap was filled with LC 5CB containing CTAB in the weight ratio 1:0.008. The LC layer thickness was 6 μm.

Figure 7.24 demonstrates the scheme of transition from the homeoplanar orientational structure to the twisted configuration. The homeoplanar director configuration was realized, owing to the different polymer films at the substrates of the LC cell. The homeotropic surface anchoring was formed at the top substrate covered with PVA–Gl film (Figure 7.24(a)). The PVA and glycerin assign the planar boundary conditions for nematic (Cognard, 1982; Volovik and Lavrentovich, 1983), but the surface-active CTA^+ cations adsorbed at the top substrate screen the orienting action of the PVA–Gl film and specify normal boundary conditions. The film of pure PVA deposited at the bottom substrate specified the planar surface anchoring for considered concentrations of CTAB in 5CB. Probably, the pure PVA exhibits a stronger planar action than the PVA containing Gl.

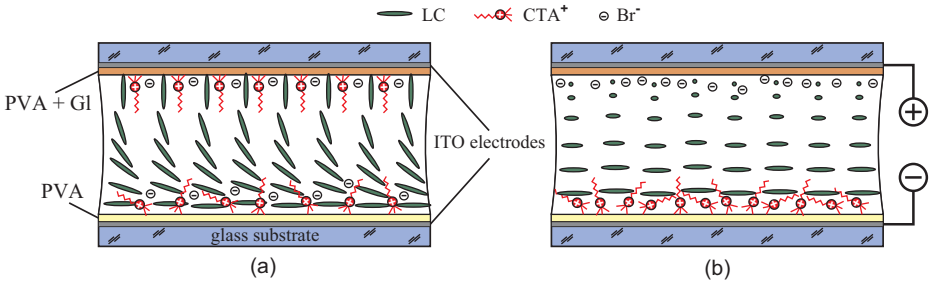

Figure 7.24: Scheme of transition of nematic layer from the homeoplanar orientational structure (a) into the twisted one (b) induced by the ionic modification of surface anchoring. (a) In the absence of electric field, the planar boundary conditions are formed at the bottom substrate while the surface anchoring at the top substrate is homeotropic. (b) The application of DC voltage with indicated polarity initiates the modification from homeotropic boundary conditions to planar one at the top substrate. At the same time, the surface anchoring at the bottom substrate is unchanged. The rubbing directions of the polymer orienting coatings are mutually orthogonal.

The applied DC electric field of suitable polarity leads to the decrease of the surface density of the CTA^+ cations at the top substrate and the planar surface anchoring is formed at this substrate (Figure 7.24(b)). The planar boundary conditions at the bottom substrate remain unchanged. As a result, the 90° twisted director configuration is realized in the LC cell due to the mutually orthogonal rubbing directions at the

substrates. The described orientational transition corresponds to the inverse regime of electrically controlled ionic modification of surface anchoring which was observed previously inside the nematic droplets (Zyryanov et al., 2008).

The changes of the optical texture of the LC layer caused by the transition from homeoplanar orientational structure to the twisted one are demonstrated in Figure 7.25. In the initial state, the LC cell placed between crossed polarizers was observed as uniform dark area when α angle between rubbing direction of the bottom substrate ($\mathbf{R}_1$) and polarizer was 0° or 90° (Figure 7.25(a) and (c), first row). The brightest optical texture appeared at $\alpha = 45°$ (Figure 7.25(b), first row). Such changes of optical texture are the evidence that the homeoplanar orientational structure was formed in the LC cell. It should be noted that the LC cell with uniform planar director configuration shows similar changes of optical textures when the sample is rotated between crossed polarizers. However, in LC cell under study the rubbing directions of orienting layers at both substrates were mutually orthogonal and, consequently, the untwisted planar configuration was unrealizable.

The optical textures of LC cell placed between crossed polarizers are not dark at any α angle when the DC voltage of 3.3 V was applied to the sample (Figure 7.25, second row). At the same time, the dark optical texture was observed in the scheme of parallel polarizers when α angle was equal to 0° or 90° (Figure 7.25(a) and (c), third row). It shows that the LC layer rotated a light polarization by 90°. Thus, the twisted director configuration was formed in the sample under the applied voltage.

It should be emphasized that the changes of LC patterns cannot be attributed to the Frederiks effect (Chandrasekhar, 1977), since the nematic 5CB has the positive dielectric anisotropy, and the electric field applied perpendicularly to the LC layer would lead to the formation of homeotropic director configuration. LC cell with such director configuration placed between crossed polarizers exhibits the dark optical pattern for any α angle. However, this disagrees with experimental observations (Figure 7.25, second row). Consequently, the observed changes of optical texture initiated by the ionic modification of boundary conditions at one of the substrates confirm the transition of nematic layer from the homeoplanar orientational structure into the twisted configuration.

Figure 7.26 shows the electro-optical response of the LC cell placed between crossed polarizers. An LC cell is controlled by square-wave monopolar (Figure 7.26(a) and (b)) and bipolar (Figure 7.26(c)) electric pulses. The positive-polarity pulse amplitude is 3.3 V and its duration is 9.8 s. For negative-polarity pulse, the amplitude is 2.2 V and its duration is 0.16 s.

The change of light transmittance of the LC cell with $\alpha = 45°$ is presented in Figure 7.25(b), and first and second rows are shown in Figure 7.26(a). The reorientation of LC induced by the ionic modification of surface anchoring leads to the change of phase retardation between two linearly polarized components of light passed through the nematic layer. For this case, the values of both on-time τ_{on} and

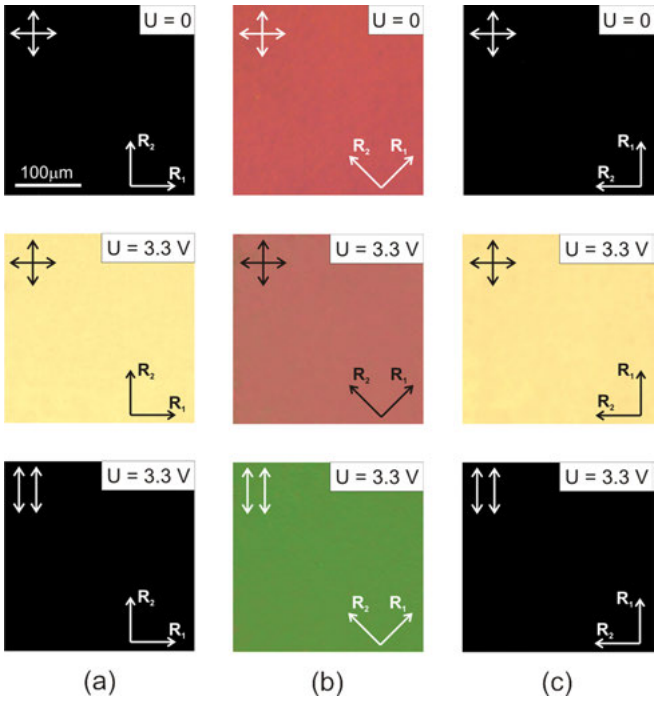

Figure 7.25: Photos of LC cell filled with 5CB containing CTAB taken in crossed polarizers scheme (first and second rows) and in parallel polarizers (third row). The α angle between the rubbing direction of the bottom substrate ($\mathbf{R}_1$) and the polarizer is 0° (a), 45° (b), and 90° (c). $\mathbf{R}_2$ is the rubbing direction of the top substrate. The first row presents the switched-off state. The second and third rows are the optical patterns under DC voltage $U = 3.3$ V.

off-time τ_{off} were close to the response times of the LC cell with transition from homeotropic director configuration to homeoplanar one (Sutormin et al., 2012, 2013).

The optical responses of the LC cell for $\alpha = 0°$ or 90° (see Figure 7.25(a) and (c), first and second rows) are presented in Figure 7.26(b) and (c). In this case, the single linearly polarized light component passes through the nematic layer. When the electric field is switched off, the light transmission of LC cell with homeoplanar orientational structure is close to zero. The positive-polarity pulse of the applied electric field leads to the formation of the twisted director configuration and the transmittance grows to 60%.

When the monopolar electric pulse is applied (Figure 7.26(b)), the values of τ_{on} and τ_{off} for LC cell with $\alpha = 0°$ or 90° are equal to 190 and 240 ms, respectively. These values are much less than the switching times both of the LC cell for $\alpha = 45°$ (Figure 7.26(a)) and the LC cell with homeotropic–homeoplanar configuration transition (Sutormin et al., 2012, 2013).

The switching-off time of the LC cell with ISO can be considerably decreased by varying the waveform of the electric pulse. For instance, the application of the bipolar electric pulse allowed decreasing τ_{off} to 11 ms (Figure 7.26(c)). When the negative-polarity electric pulse was applied to the LC cell, the CTA^+ cations returned to the top substrate faster and, consequently, the homeoplanar orientational structure was restored more rapidly.

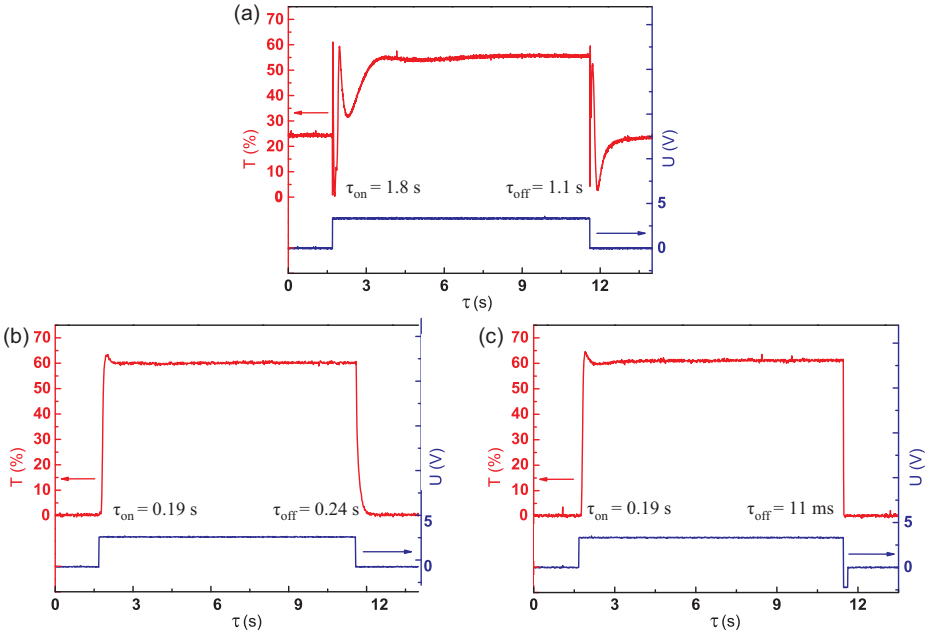

Figure 7.26: Optical responses of LC cell filled with nematic 5CB containing CTAB in crossed polarizers. The LC cell with $\alpha = 45°$ was controlled by a monopolar electric pulse (a), with $\alpha = 0°$ or 90° controlled by a monopolar electric pulse (b), and with $\alpha = 0°$ or 90° controlled by a bipolar electric pulse (c). τ_{on} and τ_{off} represent the on-time and off-time, respectively.

It should be emphasized that other methods to decrease the switching times of LC cells with ISO can be implemented; for instance, the utilization of LCs with lower viscosity and the decreasing of LC layer thickness.

7.3.4 Electrically induced anchoring transition in the ionic-surfactant-doped cholesteric layers with different confinement ratios

Electrically induced anchoring transition in the ionic-surfactant-doped cholesteric layers with confinement ratio $\rho < 1$. In this section, a reorientation of ChLC with a large helix pitch induced by the electrically controlled ionic modification of the surface anchoring

is considered (Sutormin et al., 2017). LC cells under study comprises two glass substrates with ITO electrodes coated with polymer films and the cholesteric layer between them. The polymer films based on PVA doped with glycerin compound in the weight ratio PVA:Gl = 1:0.383 were used as orienting coatings. The polymer films were deposited by spin coating and rubbed. The cell gap thickness d was set using teflon spacers and measured by means of the interference method (Huibers and Shah, 1997) with the spectrometer. Cholesteric mixtures were prepared using the nematic 5CB with the chiral additive ChA in the weight ratio of 5CB:ChA from 1:0.0030 to 1:0.0155, respectively. The nematic was preliminary doped with CTAB in the weight ratio of 5CB:CTAB = 1:0.002. The helical twisting power HTP = 6.5 μm^{-1} of the additive ChA in the nematic 5CB was determined with the droplet method (Candau et al., 1973). The used mixtures had pitch $10 \le p \le 51$ μm as calculated from $p = 1/(\mathrm{HTP} \times c_w)$, where c_w is weight concentration of the chiral agent. The confinement ratio $\rho = d/p$ in LC cells was $0.16 \le \rho \le 0.85$.

Figure 7.27 demonstrates the change of optical texture of the cholesteric layer doped with the ionic surfactant under DC voltage. In the given LC cell, the confinement ratio $\rho = 0.4$. When the electric field is switched off, the optical texture of LC layer in crossed polarizers is a uniform dark area (Figure 7.27(a)) independently of the sample rotation on the microscopic stage. Such an optical texture remains invariable until $U = 2.3$ V. The latter was accompanied with the increase in light transmission. In the range of control voltages $2.6\ \mathrm{V} \le U \le 3.4$ V, the optical texture of the cell is a uniform bright area (Figure 7.27(b)). At that, the sample rotation relative to the crossed polarizers does not lead to the dark texture. The optical textures shown in Figure 7.27(b) and (c) prove this. Here, the angle α between the rubbing direction and polarizer is 45° and 0°, respectively. Besides, at $\alpha = 0°$ (Figure 7.27(c)), the dark texture is not obtained either under the analyzer rotation. At the control voltage $U = 3.5$ V, the domains began to form in the LC cell and they appear clearly at $U = 3.7$ V (Figure 7.27(d)).

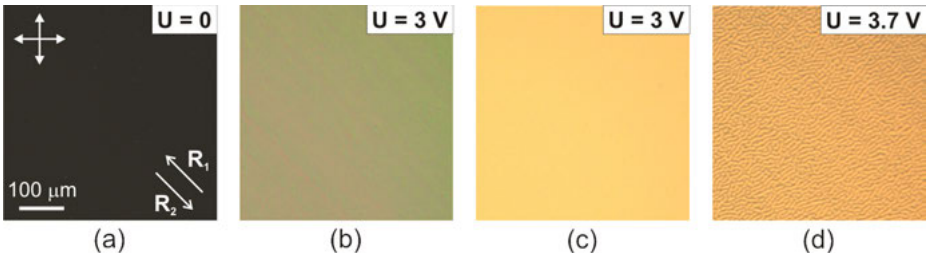

Figure 7.27: POM images of the optical textures of the cholesteric layer doped with ionic surfactant taken under variable control voltage U and α-angles between the rubbing direction of the bottom substrate ($\mathbf{R}_1$) and the polarizer: (a) $U = 0$ V, $\alpha = 45°$; (b) $U = 3$ V, $\alpha = 45°$; (c) $U = 3$ V, $\alpha = 0°$; (d) $U = 3.7$ V, $\alpha = 45°$. The cell gap thickness $d = 8.1$ μm. Confinement ratio is $\rho = 0.4$. $\mathbf{R}_2$ is the rubbing direction of the top substrate.

The similar changes of optical texture were observed in LC cells with $\rho = 0.16$ and 0.85 approximately under the same control voltage. The only difference of the initial texture of cholesteric layer with $\rho = 0.85$ is the presence of a small number of cholesteric bubbles (Kleman and Friedel, 1969). However, after the application of AC voltage, the cholesteric bubbles disappear, and the optical texture of LC layer is the uniform dark area.

The dark texture of LC layer in the absence of electric field (Figure 7.27(a)) and its invariability at the sample rotation relative to the crossed polarizers indicate a complete untwisting of the cholesteric helix and the formation of the homeotropic director orientation due to the ionic-surfactant CTAB added (Figure 7.28(a)). The cholesteric helix untwisting occurs as an effect of the normal anchoring of LC molecules with the substrates (Harvey, 1977). The formation of homeotropic or twisted structures within the cholesteric layer with rigid normal anchoring depends on the confinement ratio ρ. The transition threshold ρ_{th} value is defined by the following equation (Zel'dovich and Tabiryan, 1981):

$$\rho_{\text{th}} = K_{33}/(2K_{22}) \tag{7.6}$$

where K_{33} and K_{22} are elastic constants of the bend and twist deformations in LC, respectively. When $\rho < \rho_{\text{th}}$, the helix pitch is completely untwisted inside the LC cell with rigid normal anchoring. The twist structure is formed at $\rho > \rho_{\text{th}}$. The typical materials have the threshold value ρ_{th} of about 1 (Oswald et al., 2000). The samples under study have $\rho < 1$, which makes the helix pitch completely untwisted in the initial state.

When the DC electric field is applied, the surface anchoring on the electrode–anode substrate is modified, and the planar anchoring proper to the polymer orienting coating is restored at this substrate. The modification of the boundary conditions results in the reorientation of the LC structure and, consequently, in the change of the optical texture of the LC cell in the crossed polarizers (Figure 7.27(b)). Since the considered optical texture does not get dark completely during the sample rotation on the microscope stage relative to the crossed polarizers (Figure 7.27(b) and (c)), it means that the twisted orientational structure is formed within the LC layer. Thus, the optical textures of the LC layer presented in Figure 7.27(b) and (c) correspond to the hybrid-aligned cholesteric (HAC) structure (Belyaev et al., 1988; Dozov and Penchev, 1986; Hsiao et al., 2015; Lewis and Wiltshire, 1987; Ryabchun et al., 2015). Its orientational structure is schematically shown in Figure 7.28(b). It should be emphasized that the observable changes of optical texture cannot be induced by the Frederiks effect because the LC used in our experiment has positive dielectric anisotropy. In this case, the Frederiks effect could result only in the stabilization of the initial homeotropic director configuration.

As mentioned above, the optical texture (Figure 7.27(c)) does not become dark completely under the analyzer rotation when the polarization direction of incident

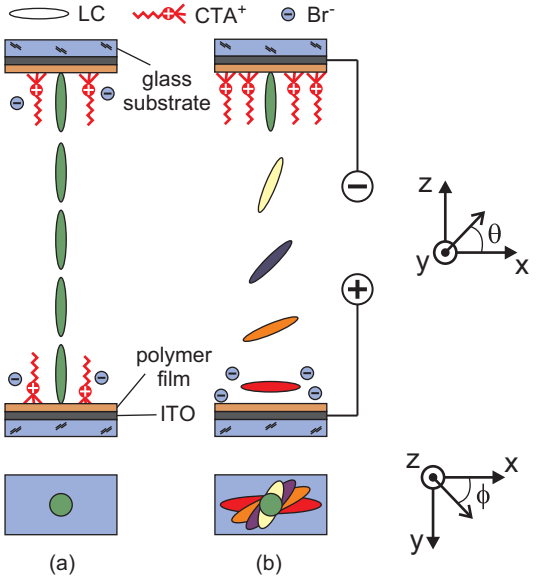

Figure 7.28: Scheme of the orientational transition induced by the DC electric field inside the cell filled with the ChLC doped by the ionic surfactant. The homeotropically aligned LC layer in initial state (a). The cholesteric layer with a hybrid structure is formed, owing to the homeotropic–planar change of surface anchoring on the electrode–anode substrate (b). θ is a tilt angle and ϕ is a twist angle. The bottom row is a top view.

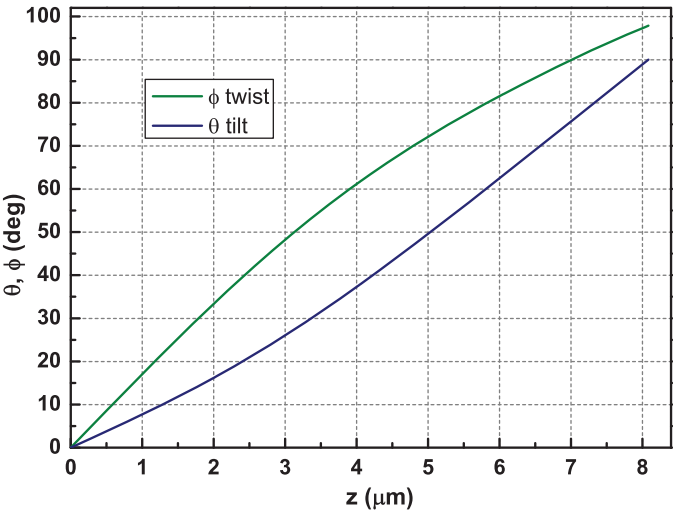

Figure 7.29: Calculation data of tilt angle θ and twist angle ϕ of the director versus the z-coordinate perpendicular to the cell substrates for the hybrid-aligned cholesteric structure. $z = 0$ and $z = 8.1$ μm correspond to the substrates with planar and homeotropic surface anchoring, respectively. Thickness of the LC layer is $d = 8.1$ μm. The helix pitch is $p = 21$ μm.

light coincides with the substrate rubbing direction. It indicates that the light after passing through the layer of hybrid-aligned ChLC is no longer linearly polarized. The light polarization change for such a system has been simulated. First, the cholesteric orientational structure within the cell was calculated by means of the energy minimization of elastic deformations of the director field (Timofeev et al., 2012) under asymmetric boundary conditions. The LC surface anchoring on one of the substrates was planar and another one was homeotropic. Then applying the Berreman 4×4-matrix method (Berreman, 1972), the light polarization after the LC-layer transmission was simulated. The following parameters of 5CB were used for the calculations: the elastic constants of the splay deformation $K_{11} = 5.7$ pN, the twist deformation $K_{22} = 3.5$ pN, and the bend deformation $K_{33} = 7.7$ pN (Cui and Kelly, 1999b); the extraordinary and ordinary refractive indices $n_e = 1.7002$, $n_o = 1.5294$ ($\lambda = 632.8$ nm), respectively (Bunning et al., 1986); the thickness of LC layer $d = 8.1$ μm, the helix pitch $p = 21$ μm, and the confinement ratio $\rho = 0.4$.

Figure 7.29 shows the calculation data for the hybrid-aligned cholesteric structure. The simultaneous tilt and twist of the director are shown to occur inside the LC layer. The total twist angle of director is 98°. The Berreman method simulation has revealed that the linearly polarized light beam ($\lambda = 632.8$ nm) passing through such an LC orientational structure gets elliptically polarized. The ratio of major axis to minor axis of the polarization ellipse is 3.8. At that, the β angle between the polarization direction of incident light and the major axis of elliptically polarized light is 68° when leaving the LC layer.

We measured β angle depending on the control voltage value. The cell was placed between the crossed polarizers so that the rubbing direction of input substrate coincided with the polarization direction of incident He–Ne laser beam. After that, the DC voltage was applied to the LC cell. When the light transmission reached the saturation, which corresponds to the formation of the hybrid-aligned ChLC, the minimal light transmission of the system was found by means of the analyzer rotation. In this case, the direction of major axis of the elliptically polarized light was perpendicular to the analyzer direction. In the range 2.6–3.2 V of control voltages, β angle changed from 62° to 64°, respectively. These data are in good accordance with the calculated results.

Figure 7.30 shows the oscillograms of the square-wave response of the LC cell placed between crossed polarizers. The pulse amplitude is 2.6 V and its duration is 10 s. The oscillogram in Figure 7.30(a) corresponds to the situation when the polarization of incident light coincides with the rubbing direction ($\alpha = 0°$), and $\alpha = 45°$ in Figure 7.30 (b). In the initial state, the light transmission of the system is close to zero because of the homeotropic director orientation. The applied electric pulse increases the light transmission caused by the formation of the HAC structure. If the polarization of incident light coincides with the rubbing direction (Figure 7.30(a)), the light transmission saturation reaches 58%. The on-time τ_{on} was 0.31 s, and the off-time τ_{off} was 0.51 s. For $\alpha = 45°$, the transmittance saturation reached 51% (Figure 7.30(b)),

$\tau_{on} = 0.13$ s, $\tau_{off} = 0.59$ s. Under the control voltages $2.6 \le U \le 3.2$ V, the on-time τ_{on} did not practically change. The off-time τ_{off} in the same range of voltages increased up to 1.75 s. It should be noted that the change in the control pulse form is able to lead to a significant improvement of the dynamic characteristics of an LC cell with electrically controlled ionic modification of the surface anchoring (Sutormin et al., 2014).

Electrically induced anchoring transition in the ionic-surfactant-doped cholesteric layers with confinement ratio $\rho > 1$. We considered also a change of ChLC orientation initiated by the ionic modification of boundary conditions in the layers with confinement ratio $\rho > 1$ (Sutormin et al., 2018b). The investigations were performed with the same LC cells as in the previous section. The substrates of the cells were covered by the polymer films using spin coating technique and then these layers were unidirectionally rubbed. The polymer films were PVA containing glycerin compound (Gl) in the weight ratio PVA:Gl = 1:0.479. The cholesteric under study was a mixture of nematic 5CB and ChA in the weight ratio ranging between 1:0.0233 and 1:0.0658. In addition, ChLC contained ionic-surfactant CTAB in a weight ratio 5CB:CTAB = 1:0.0041. In the utilized mixtures, the intrinsic cholesteric pitch varied from 2.6 to 7.1 μm, and the confinement ratio was $1.2 \le \rho \le 8$. Filling of cells was performed with ChLC in the isotropic phase. The diffraction patterns were observed utilizing He–Ne laser with wavelength $\lambda = 632.8$ nm.

At first, the reorientation of the director in LC cells under application of the 1 kHz AC voltage was studied. The optical patterns of the ChLC layer with the confinement ratio $\rho = 1.2$ observed for several values of the applied AC voltage are presented in Figure 7.31. The intrinsic pitch p was 7.1 μm and the ChLC thickness $d = 8.2$ μm. In the absence of electric field the fingerprint pattern is observed (Figure 7.31(a)). When AC voltage is applied to the sample, the initial optical texture changes gradually into a dark area (Figure 7.31(b)–(d)). It should be noted that the rotation of the sample between two crossed polarizers does not lead to the changing of dark optical pattern.

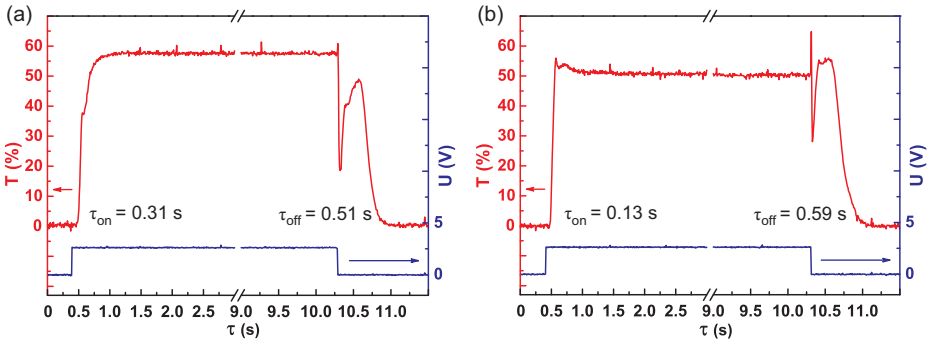

Figure 7.30: Optical response of the LC cell filled with the ionic-surfactant-doped cholesteric layers in crossed polarizers at different α-angles between the polarizer and the rubbing direction: (a) $\alpha = 0°$; (b) $\alpha = 45°$. Applied voltage amplitude is 2.6 V. Confinement ratio is $\rho = 0.4$.

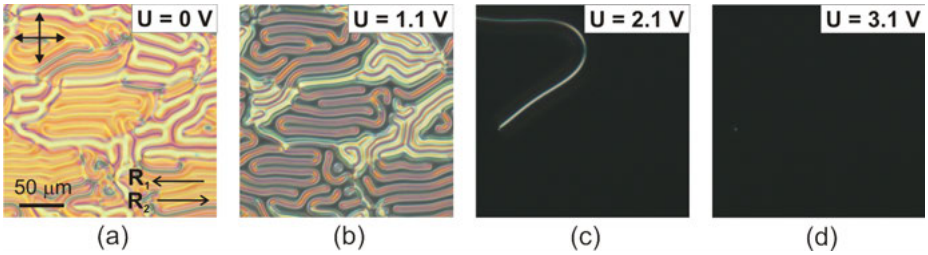

Figure 7.31: Photos taken in crossed polarizers of the cholesteric layer with the ionic surfactant additive for AC voltages $U = 0$ V (a), 1.1 V (b), 2.1 V (c), and 3.1 V (d). The intrinsic cholesteric pitch $p = 7.1$ μm. Confinement ratio $\rho = 1.2$. The rubbing directions of the bottom and top substrates are marked by $\mathbf{R}_1$ and $\mathbf{R}_2$, hereinafter.

As stated above, depending on the ratio d/p the untwisted or twisted ChLC orientational structures in the cell with rigid homeotropic boundary conditions can be realized. The transition between these configurations occurs at the critical value of d/p, which is assigned by the ratio of elastic constants for bend and twist deformations (Zel'dovich and Tabiryan, 1981). In typical LC substances, the critical value of d/p is about 1 (Oswald et al., 2000) and for this reason, the fingerprint pattern corresponding to the twisted director configuration was realized in the sample with $\rho = 1.2$ (Figure 7.31(a)).

Applied AC voltage initiates the reorientation of LC director along the electric field owing to the positive dielectric anisotropy of the cholesteric. This process leads to the transition of twisted ChLC alignment into the homeotropic orientational structure whose optical pattern is demonstrated in Figure 7.31(d). The similar change of director configuration occurred in other samples with ρ ranging between 1.2 and 8. The higher AC voltage was necessary to produce the homeotropic orientational structure in samples with larger values of confinement ratio. Furthermore, in some samples, the AC voltage initiated the hydrodynamic flows, which led to the formation of particular optical textures (Figure 7.32) like the ones demonstrated by Ribiére et al. (1994).

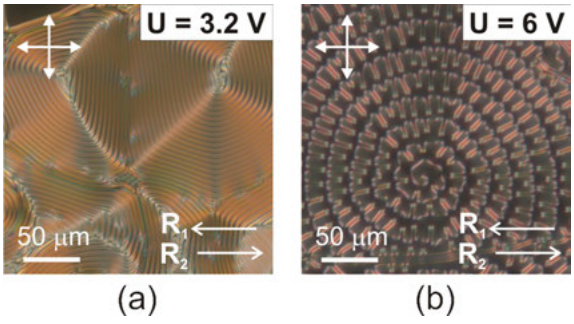

Figure 7.32: Photos taken in crossed polarizers of the cholesteric layers with the ionic-surfactant additive under application of an AC voltage. (a) $\rho = 1.9$ and $U = 3.2$ V; (b) $\rho = 3.2$ and $U = 6$ V.

Completely different changes of the ChLC optical pattern were observed under the action of a DC electric field (Figure 7.33). In the initial state, the fingerprint texture is realized (Figure 7.33(a)). When the value of applied DC voltage is smaller than 2.7 V, the fingerprint texture does not change. The striped domain structure with defects is formed in the range of DC voltage from 2.7 to 3.3 V (Figure 7.33(b)–(d)). A higher value of DC voltage leads to the appearance of domains that are due to electrohydrodynamic instability in cholesteric layers. A number of defects in the striped domain structure can be decreased considerably using the preliminary action of AC voltage pulse.

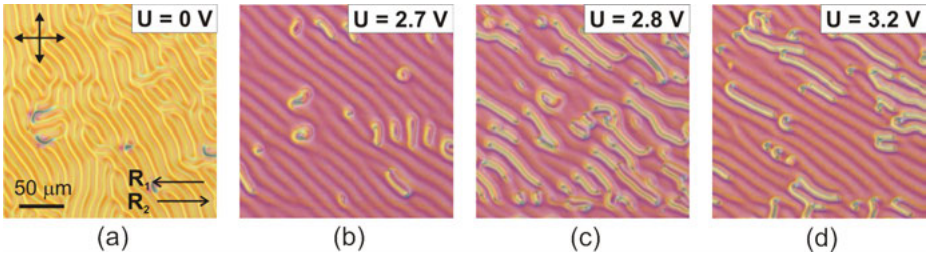

Figure 7.33: Photos taken in crossed polarizers of the cholesteric layer with the ionic-surfactant additive for DC voltages $U = 0$ V (a), 2.7 V (b), 2.8 V (c), and 3.2 V (d). The intrinsic cholesteric pitch $p = 7.1$ μm. Confinement ratio $\rho = 1.2$.

As an example, Figure 7.34 demonstrates the striped domain structures realized under DC voltage $U = 3.0$ V with and without preliminary action of 1 kHz AC voltage of 10.3 V value. Obviously, in the case of preliminary action of AC voltage, the number of defects in the striped domain structure decreased considerably. The transformations of ChLC optical texture presented in Figure 7.33 are initiated by the modification of boundary conditions at the anode–substrate. Initially, the normal surface anchoring of cholesteric layer is realized on both substrates due to the adsorbed CTA^+ cations. Applied DC electric field causes decreasing the surface density of CTA^+ cations at the anode–substrate. As a result, the tangential surface anchoring specifying the polymer layer is formed at this substrate and the director configuration inherent in HAC layer is realized in the bulk. Depending on the ratio between ChLC thickness and cholesteric pitch, the director configuration of uniform HAC (UHAC) or modulated HAC (MHAC) structure can be appeared in the layer with asymmetric boundary conditions (Dozov and Penchev, 1986b). The simultaneous twist and tilt of director takes place along the normal to the substrates in the orientational structure of HAC. LC orientation in the plane of the layer is uniform in the case of UHAC director configuration. But in the MHAC structure, the surface layer with periodically distorted cholesteric helix axis is formed near the substrate with normal surface anchoring (Baudry et al., 1996; Dozov and Penchev, 1986).

For this reason, the cholesteric layers with UHAC and MHAC director configurations exhibit the different optical textures. The cholesteric with UHAC director configuration appears as a uniform bright area, whereas the optical texture of ChLC with MHAC director configuration is a stripe domain pattern and orientation of domains is specified by the confinement ratio (Baudry et al., 1996; Belyaev et al., 1988; Dozov and Penchev, 1986; Lin et al., 2012; Nose et al., 2010; Ryabchun et al., 2015). It was shown by Belyaev et al. (1988) that the change between UHAC and MHAC director configuration occurs at the confinement ratio of about 1 and this agrees with our experimental data.

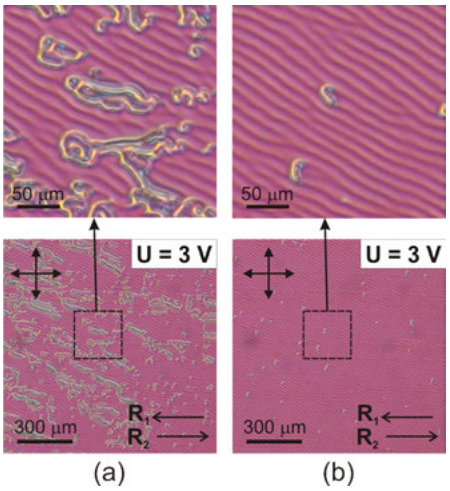

Figure 7.34: Photos taken in crossed polarizers of the cholesteric layer containing the ionic-surfactant additive for DC voltage $U = 3.0$ V without the preliminary action of AC electrical field (a) and with the preliminary effect of 1 kHz AC electrical field of 10.3 V value (b). The scaled-up parts of LC textures are shown in the top row. The intrinsic cholesteric pitch $p = 7.1$ μm and confinement ratio $\rho = 1.2$.

The electrically controlled ionic modification of boundary conditions induced the appearance of UHAC director configuration in the samples with $\rho < 1$ and the optical pattern of ChLC layer looked like a uniform bright area (Sutormin et al., 2017b). In LC layer with $\rho = 1.2$, the application of DC voltage (Figures 7.33 and 7.34) initiated the formation of MHAC director configuration, and the stripe domain pattern was observed.

Figure 7.35 demonstrates the change of optical pattern of ChLC layer under the action of DC electric field in the sample with a confinement ratio $\rho = 1.9$. It is seen that the transformation of the pattern is similar to the observed changes in the sample with $\rho = 1.2$. The initial optical pattern does not change when the value of applied DC voltage is smaller than 2.6 V. The striped domain texture with defects is formed in the range of DC voltages from 2.7 to 3.4 V. But a number of defects were

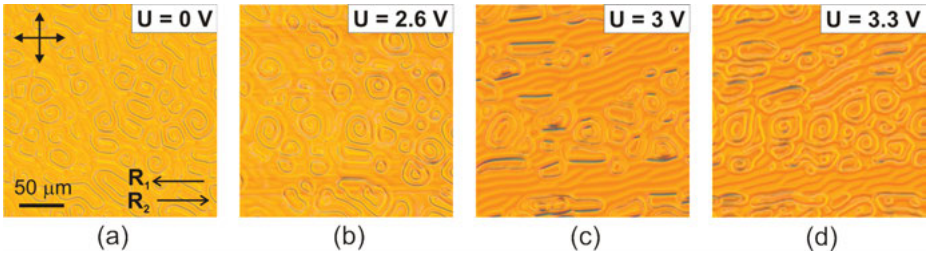

Figure 7.35: Photos taken in crossed polarizers of the cholesteric layer with the ionic-surfactant additive for DC voltages $U = 0$ V (a), 2.6 V (b), 3.0 V (c), and 3.3 V (d). The intrinsic cholesteric pitch $p = 4.2$ μm, and confinement ratio $\rho = 1.9$.

greater than the sample with confinement ratio $\rho = 1.2$, and a high-quality stripe domain pattern could not be formed utilizing the preliminary influence of AC voltage.

In the sample with confinement ratio $\rho = 3.2$ (Figure 7.36), the director reorientation process initiated by the ionic modification of boundary conditions starts from the DC voltage $U = 2.7$ V, whose value is close to the threshold voltages in samples with $\rho = 1.2$ and 1.9. One can see that the layer areas with a periodic stripe domain texture are very small (Figure 7.36(c)). In the sample with confinement ratio $\rho = 8$, the action of DC electric field did not initiate the visible transformations of optical pattern at all.

Lin et al. (2012) experimentally showed that the MHAC director configuration appears as high-quality stripe domain pattern only in a narrow range of the confinement ratios. When the confinement ratio exceeded the upper range limit, a large number of defects were observed in the stripe domain pattern. It was proposed that the strength of tangential surface anchoring became insufficient to produce a defect-free structure (Lin et al., 2012). This is probably the reason for the formation of the striped domain pattern with a different number of defects in our investigated samples. Besides, the observed striped domain pattern had more defects in the samples with higher values of confinement ratio.

The dynamic characteristics of the LC cell driven by ionic-surfactant method are specified by a number of processes such as the motion of CTA^+ cations, the modification of boundary conditions, and the change of LC orientation in the layer (Sutormin et al., 2012). The on-time and off-time of investigated cholesteric cells were of the order of 1 s. These dynamic characteristics agreed with the response times of nematic cells driven by the ionic-surfactant method (Sutormin et al., 2012, 2013).

It is known that the MHAC structure is suitable to produce the diffraction grating, which can be controlled by the electric field, light radiation, or temperature (Lin et al., 2012; Nose et al., 2010; Ryabchun et al., 2015). The external actions change the cholesteric pitch and initiate the rotation of the stripe domains. For this reason, it is interesting to investigate the diffraction patterns obtained after passing the laser beam through the cholesteric cell with ISO. The sample with confinement ratio $\rho = 1.2$ was examined. To obtain the high-quality stripe domain pattern (Figure 7.34(b)), the preliminary

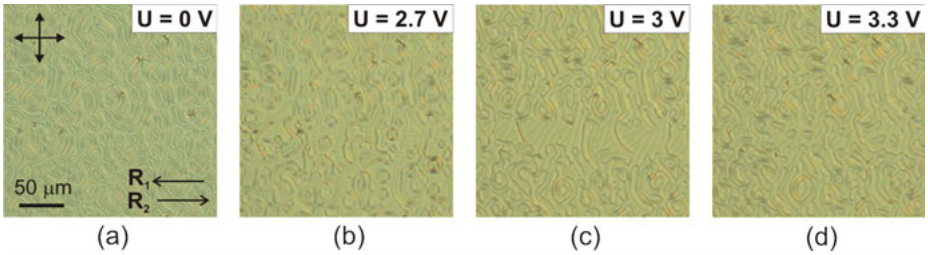

Figure 7.36: Photos taken in crossed polarizers of the cholesteric layer with the ionic-surfactant additive for DC voltages $U = 0$ V (a), 2.7 V (b), 3.0 V (c), and 3.3 V (d). The intrinsic cholesteric pitch $p = 2.6$ µm, and confinement ratio $\rho = 3.2$.

action of 1 kHz AC voltage of 10.3 V was used. Figure 7.37 presents the change in diffraction pattern initiated by the applied DC voltage $U = 3.0$ V. In the initial state, the diffraction pattern was concentric rings (Figure 7.37(a)) owing to the fingerprint texture without preferred domain orientation was formed in the sample (Figure 7.33 (a)). Applied DC voltage initiated the formation of optical texture containing the stripe domains (Figure 7.34(b)), and the diffraction pattern changed to a set of three light reflexes (Figure 7.37(b)). The diffraction pattern remained almost unchanged in the range of applied voltages from 2.7 to 3.2 V, and it was the evidence that the rotation of stripe domains did not occur. Consequently, a switching between only two diffraction patterns can be obtained by using the ionic modification of boundary conditions.

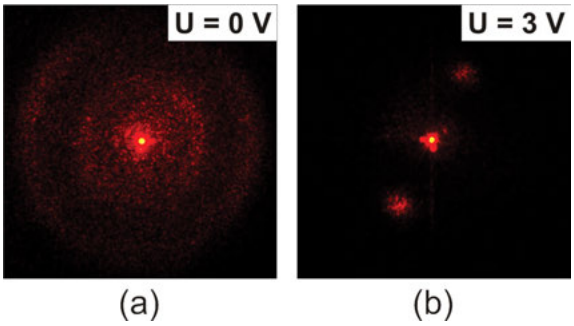

Figure 7.37: Change of diffraction pattern behind the ChLC layer under the application of DC voltage. (a) $U = 0$ V and (b) $U = 3.0$ V. The intrinsic cholesteric pitch $p = 7.1$ µm, and confinement ratio $\rho = 1.2$.

7.4 Conclusions

In this chapter, we have demonstrated that the ISO method can be successfully applied to the state switching of NLCs and ChLCs irrespective of both the value and sign of their dielectric anisotropy $\Delta\varepsilon$, and it is even applicable to LCs with $\Delta\varepsilon = 0$. It is well known that zero-$\Delta\varepsilon$ LCs cannot in principle be controlled by the classical Frederiks effect. Apart from the LC systems, the ISO method has been proved to be suitable for the operation of polymer/LC composite systems such as PDLC films, where a modification of boundary conditions can be realized in both the normal and inverse modes depending on the content of ionic surfactant in LC.

The values of the response times for the ISO method take several seconds or tens of seconds. But these parameters can be improved by several ways. For example, one may choose LC with low viscosity because the well-known LCs 5CB and MBBA exemplarily discussed in this chapter are not optimal materials regarding this aspect. Ion transport velocity under the action of electric field in low-viscosity LCs will increase and hence the response times will drop. Another approach is to use the orientational transition between the homeoplanar configuration and the twisted structure in a nematic layer. As shown above, the response times decrease in this case to some hundreds of milliseconds. If to apply additionally the opposite pulse before the field is turned off, the relaxation time decreases to 11 μs.

In cholesteric layers with a confinement ratio in the range of 0.16–0.85, the DC electric field induced the transition from the homeotropic director configuration to the UHAC structure. The on-time for such LC cells was tenth parts of a second and off-time was about a second. Initially, the fingerprint texture was realized in the LC cells with confinement ratios exceeding 1. The DC electric field induced the formation of MHAC structure whose optical texture appeared as periodic stripes.

Obviously, the ISO method for switching LC states has its pros and cons. A few drawbacks can be listed, including the slower electro-optical response in comparison with that of the similar orientational transitions induced by the Frederiks effect, and the probable electrochemical degradation of the substrates and LC structures. Among the advantages, the method allows operating various surface phenomena in plasmonics, light reflection, and others; the method practically depends neither on the value nor the sign of LC dielectric anisotropy; this method requires a small value of control voltage; it enables low power consumption of LC structures with novel types of bistability effects; the special production technologies are not required because the manufacturing lines for conventional LC displays can be used to produce the LC devices controlled by the ionic-surfactant method. All these allow believing that the development of this approach can lead to the creation of principally new LC materials capable of significantly expanding the functional possibilities of optoelectronic LC devices.

References

Barannik, A., Shabanov, V., Zyryanov, V., Lapanik, V., Bezborodov, V. (2005). Interference and ion effects in the electro-optical response of PDNLC films. Journal of the Society for Information Display, 13, 273–279.

Barbero, G., Evangelista, L.R. (2006). Adsorption Phenomena and Anchoring Energy in Nematic Liquid Crystals, Taylor and Francis, Boca Raton, 352.

Baudry, J., Brazovskaia, M., Lejcek, L., Oswald, P., Pirkl, S. (1996). Arch-texture in cholesteric liquid crystals. Liquid Crystals, 21(6), 893–901.

Belyaev, S.V., Barnik, M.I., Beresnev, G.A., Malimonenko, N.V. (1988). Optical and electrooptical properties of homeoplanar layers of cholesteric liquid crystals. Liquid Crystals, 3, 1279–1282.

Berreman, D.W. (1972). Optics in stratified and anisotropic media: 4×4-matrix formulation. Journal of the Optical Society of America, 62(4), 502–510.

Berreman, D.W., Heffner, W.R. (1981). New bistable liquid-crystal twist cell. Journal of Applied Physics, 52, 3032–3039.

Blinov, L.M. (1983). Electro-Optical and Magneto-Optical Properties of Liquid Crystals, Wiley, New York, 384.

Blinov, L.M. (2011). Structure and Properties of Liquid Crystals, Springer, Dordrecht, Heidelberg, London, New York.

Blinov, L.M., Chigrinov, V.G. (1993). Electrooptic Effects in Liquid Crystal Materials, Springer, New York.

Blinov, L.M., Davydova, N.N., Sonin, A.A., Yudin, S.G. (1984). The local frederiks transition in nematic liquid crystals. Kristallografiya, 29(3), 537–541.

Blinov, L.M., Kats, E.I., Sonin, A.A. (1987). Surface physics of thermotropic liquid crystals. Soviet Physics-Uspekhi, 30(7), 604–619.

Born, M., Wolf, E. (1999). The Principles of Optics. Nauka, Moscow, Vol. 1973, 6th ed., Cambridge Univ. Press, Cambridge.

Bradshaw, M.J., Raynes, E.P., Bunning, J.D., Bunning, J.D., Faber, T.E. (1958). The Frank constants of some nematic liquid crystals. Journal de Physique, 46(9), 1513–1520.

Bunning, J.D., Crellin, D.A., Faber, T.E. (1986). The effect of molecular biaxiality on the bulk properties of some nematic liquid-crystals. Liquid Crystals, 1(1), 37–51.

Bunning, J.D., Faber, T.E., Sherrell, P.L. (1981). The Frank constants of nematic 5CB at atmospheric pressure. Journal de Physique, 42(8), 1175–1182.

Candau, S., Le Roy, P., Debeauvais, F. (1973). Magnetic field effects in nematic and cholesteric droplets suspended in a isotropic liquid. Molecular Crystals and Liquid Crystals, 23, 283–297.

Chandrasekhar, S. (1977). Liquid Crystals, Raman Research Institute, Cambridge Univ. Press, Cambridge, 1977; Mir, Moscow, 1980.

Cognard, J. (1982). Alignment of Nematic Liquid Crystals and Their Mixtures, Gordon and Breach, Paris, 104.

Crawford, G.P., Zumer, S. (1996). Liquid Crystals in Complex Geometries, Taylor and Francis, London, 584.

Cui, M., Kelly, J.R. (1999). Temperature dependence of visco-elastic properties of 5CB. Molecular Crystals and Liquid Crystals, 331, 1909–1917.

Doane, J.W. (1991). Polymer-dispersed liquid-crystals-boojums at work. MRS Bulletin, 16, 22–28.

Dozov, I., Penchev, I. (1986). Structure of a hybrid aligned cholesteric liquid crystal cell. Journal de Physique France, 47, 373–377.

Drzaic, P.S. (1995). Liquid Crystal Dispersions, World Scientific, Singapore, 429.

Dubois-Violette, E., De Gennes, P.G. (1975). Local Frederiks transitions near a solid/nematic interface. Journal de Physique Letters, 36(10), L255–L258.

Fréedericksz, V., Tsvetkov, V. (1935). Concerning the orienting action of an electric field on molecules of anisotropic liquids. Doklady Akademii Nauk SSSR, 2, 528–531.
Freedericksz, V.K., Zolina, V. (1933). Forces causing the orientation of an anisotropic liquid. Transactions of the Faraday Society, 29, 919–930.
Gardymova, A.P., Zyryanov, V.Y., Loiko, V.A. (2011). Multistability in polymer-dispersed cholesteric liquid crystal film doped with ionic surfactant. Technical Physics Letters, 37(9), 805–808.
Grawford, G.P. (2005). Flexible Flat Panel Displays, John Wiley & Sons, Hoboken.
Greubel, W. (1974). Bistability behavior of texture in cholesteric liquid crystals in an electric field. Applied Physics Letters, 25, 5–7.
Harvey, T.B. (1977). A boundary induced cholesteric-nematic phase transition. Molecular Crystals and Liquid Crystals, 34, 225–229.
Hsiao, Y.-C., Timofeev, I.V., Zyryanov, V.Y., Lee, W. (2015). Hybrid anchoring for a color-reflective dual-frequency cholesteric liquid crystal device switched by low voltages. Optical Materials Express, 5(11), 2715–2720.
Hsu, J.S., Liang, B.J., Chen, S.H. (2004). Bistable chiral tilted-homeotropic nematic liquid crystal cells. Applied Physics Letters, 85, 5511–5513.
Huibers, P.D.T., Shah, D.O. (1997). Multispectral determination of soap film thickness. Langmuir, 13, 5995–5998.
Kleman, M., Friedel, J. (1969). Lignes de Dislocation Dans les Cholestériques. Journal de Physique. Colloques 30 (Suppl. C4), 43, C4-43–C4-53.
Klingbiel, R.T., Genova, D.J., Bucher, H.K. (1974). The temperature dependence of the dielectric and conductivity anisotropies of several liquid crystalline materials. Molecular Crystals and Liquid Crystals, 27, 1–21.
Komitov, L., Helgee, B., Felix, J., Matharu, A. (2005). Electrically commanded surfaces for nematic liquid crystal displays. Applied Physics Letters, 86(2), 023502.
Krakhalev, M.N., Loiko, V.A., Zyryanov, V.Y. (2011). Electro-optical characteristics of polymer-dispersed liquid crystal film controlled by ionic-surfactant method. Technical Physics Letters, 37, 34–36.
Krakhalev, M.N., Prishchepa, O.O., Zyryanov, V.Y. (2009). Inverse mode of ion-surfactant method of director reorientation inside nematic droplets. Molecular Crystals and Liquid Crystals, 512, 1998–2003.
Lewis, M.R., Wiltshire, C.K. (1987). Hybrid aligned cholesteric: a novel liquid-crystal alignment. Applied Physics Letters, 51, 1197–1199.
Lin, C.-H., Chiang, R.-H., Liu, S.-H., Kuo, C.-T., Huang, C.-Y. (2012). Rotatable diffractive gratings based on hybrid-aligned cholesteric liquid crystals. Optics Express, 20(20), 26837–26844.
Meyer, R.B. (1972). Point disclinations at a nematic-isotropic liquid interface. Molecular Crystals and Liquid Crystals, 16, 355–369.
Nose, T., Miyanishi, T., Aizawa, Y., Ito, R., Honma, M. (2010). Rotational behavior of stripe domains appearing in hybrid aligned chiral nematic liquid crystal cells. Japanese Journal of Applied Physics, 49, 051701.
Ondris-Crawford, R., Boyko, E.P., Wagner, B.G., Erdmann, J.H., Zumer, S., Doane, J.W. (1991). Microscope textures of nematic droplets in polymer dispersed liquid crystals. Journal of Applied Physics, 69(9), 6380–6386.
Oswald, P., Baudry, J., Pirkl, S. (2000). Static and dynamic properties of cholesteric fingers in electric field. Physics Reports, 337, 67–96.
Petrov, A.G., Durand, G. (1994). Electric field transport of biphilic ions and anchoring transitions in nematic liquid crystals. Liquid Crystals, 17(4), 543–554.
Prishchepa, O.O., Shabanov, A.V., Zyryanov, V.Y. (2005). Director configurations in nematic droplets with inhomogeneous boundary conditions. Physical Review E, 72, 031712.

Prishchepa, O.O., Shabanov, A.V., Zyryanov, V.Y., Parshin, A.M., Nazarov, V.G. (2006). Friedericksz threshold field in bipolar nematic droplets with strong surface anchoring. Journal of Experimental and Theoretical Physics Letters, 84(11), 607–612.

Proust, J.E., Ter Minassian Saraga, L. (1972). Orientation of a nematic liquid crystal by suitable boundary surfaces. Solid State Communications, 11(9), 1227–1230.

Ribiére, P., Oswald, P., Pirkl, S. (1994). Crawling and spiraling of cholesteric fingers in electric field. Journal de Physique II, 4(1), 127–143.

Ryabchun, A., Bobrovsky, A., Stumpe, J., Shibaev, V. (2015). Rotatable diffraction gratings based on cholesteric liquid crystals with phototunable helix pitch. Advanced Optical Materials, 3(9), 1273–1279.

Ryschenkow, G., Kleman, M. (1976). Surface defects and structural transitions in very low anchoring energy nematic thin films. The Journal of Chemical Physics, 64, 404–412.

Skarp, K., Lagerwall, S.T., Stebler, B. (1980). Measurements of hydrodynamic parameters for nematic 5CB. Molecular Crystals and Liquid Crystals, 60(3), 215–236.

Sutormin, V.S., Krakhalev, M.N., Prishchepa, O.O., Lee, W., Zyryanov, V.Y. (2014). Electro-optical response of an ionic-surfactant-doped nematic cell with homeoplanar–twisted configuration transition. Optical Materials Express, 4(4), 810–815.

Sutormin, V.S., Krakhalev, M.N., Prishchepa, O.O., Zyryanov, V.Y. (2012). Electrically controlled local fredericksz transition in a layer of a nematic liquid crystal. Journal of Experimental and Theoretical Physics Letters, 96, 511–516.

Sutormin, V.S., Krakhalev, M.N., Zyryanov, V.Y. (2013). The dynamics of the response of an electro-optic cell based on a nematic layer with controlled surface anchoring. Technical Physics Letters, 39(7), 583–586.

Sutormin, V.S., Timofeev, I.V., Krakhalev, M.N., Prishchepa, O.O., Zyryanov, V.Y. (2017). Orientational transition in the cholesteric layer induced by electrically controlled ionic modification of the surface anchoring. Liquid Crystals, 44(3), 484–489.

Sutormin, V.S., Timofeev, I.V., Krakhalev, M.N., Prishchepa, O.O., Zyryanov, V.Y. (2018). Electrically induced anchoring transition in cholesteric liquid crystal cells with different confinement ratios. Liquid Crystals, 45(8), 1129–1136.

Timofeev, I.V., Lin, Y.-T., Gunyakov, V.A., Myslivets, S.A., Arkhipkin, V.G., Vetrov, S.Y., Lee, W., Zyryanov, V.Y. (2012). Voltage-induced defect mode coupling in a one-dimensional photonic crystal with a twisted-nematic defect layer. Physical Review E, 85(1), 011705.

Volovik, G.E., Lavrentovich, O.D. (1983). Topological dynamics of defects: boojums in nematic drops. Journal of Experimental and Theoretical Physics, 58(6), 1159–1166.

Yang, D.K. (2006). Flexible bistable cholesteric reflective displays. Journal of Display Technology, 2, 32–37.

Yang, D.K., Huang, X.Y., Zhu, Y.M. (1997). Bistable cholesteric reflective displays: materials and drive schemes. Annual Review Materials Science, 27, 117–146.

Zel'dovich, B.Y., Tabiryan, N.V. (1981). Freedericksz transition in cholesteric liquid crystals without external fields. Journal Experimental and Theoretical Physics Letters, 34, 428–430.

Zharkova, G.M., Sonin, A.S. (1994). Mesomorphic composites. Nauka, Novosibirsk, 214.

Zumer, S., Doane, J.W. (1986). Light scattering from a small nematic droplet. Physical Review A, 34(4), 3373–3386.

Zyryanov, V.Y., Krakhalev, M.N., Prishchepa, O.O., Shabanov, A.V. (2007). Orientational structure transformations caused by the electric-field-induced ionic modification of the interface in nematic droplets. Journal of Experimental and Theoretical Physics Letters, 86(6), 383–388.

Zyryanov, V.Y., Krakhalev, M.N., Prishchepa, O.O., Shabanov, A.V. (2008). Inverse regime of ionic modification of surface anchoring in nematic droplets. Journal of Experimental and Theoretical Physics Letters, 88(9), 597–601.

Zyryanov, V.Y., Smorgon, S.L., Zhuikov, V.A., Shabanov, V.F. (1994). Memory effects in polymer-encapsulated cholesteric liquid-crystals. Journal of Experimental and Theoretical Physics Letters, 59, 547–550.

Zyryanov, V.Y., Zhuikov, V.A., Smorgon, S.L., Shabanov, V.F. (1996). Thermooptical recording of information in polymer-capsulated cholesteric liquid crystals. Technical Physics, 41(8), 799–802.